UC Berkeley
UC Berkeley Electronic Theses and Dissertations

Title

Plasticity in the Auditory Pathway

Permalink

https://escholarship.org/uc/item/3x52k142

Author

Miyakawa, Asako

Publication Date

2014

Peer reviewed|Thesis/dissertation

eScholarship.org Powered by the California Digital Library
University of California

Plasticity in the Auditory Pathway

By

Asako Miyakawa

A thesis submitted in partial satisfaction of the

requirements for the degree of

Doctor of Philosophy

in

Neuroscience

in the

GRADUATE DIVISION

of the

UNIVERSITY OF CALIFORNIA, BERKELEY

Committee in charge:

Professor Shaowen Bao, Chair
Professor Yang Dan
Professor Daniel Feldman
Professor Keith Johnson

Fall 2014

Copy Right 2014

Asako Miyakawa

All Rights Reserved

Abstract

Plasticity in the Auditory Pathway

by Asako Miyakawa

Doctor of Philosophy in Neuroscience

University of California, Berkeley

Professor Shaowen Bao, Chair

The auditory pathway has a remarkable ability to change its response based on sound experiences. Plasticity also occurs as an adaptive response following injury to the auditory pathway, such as in hearing loss. My doctoral work aims to improve our understanding of plasticity in the auditory system during normal development, and in cases of trauma or disease.

First, I studied the tonotopic map of the primary auditory cortex and inferior colliculus in juvenile rats that underwent passive exposure to a single frequency pure tone pip during the auditory critical period. Previously it has been shown that such acoustic exposure leads to an enlarged representation of the exposure frequency in primary auditory cortex. However, whether this change originated in cortex or also present in an upstream auditory nucleus remained unclear. I addressed this question by comparing the tonotopic representations of inferior colliculus and primary auditory cortex and showed that enlarged frequency representation is observed only in the primary auditory cortex but not in the inferior colliculus.

Second, I investigated adult plasticity following hearing loss. It has been hypothesized that a reorganization of auditory cortex underlies perceptual problems that develop after hearing loss. In particular, perception of a phantom sound, or tinnitus, has been associated with abnormal tonotopic representation in the auditory cortex. Using a mouse behavioral model of tinnitus, I have shown that tonotopic map reorganization is likely a consequence of hearing loss, and is not sufficient to induce tinnitus by itself. Further, I have provided evidence that changes in the Glutamate Decarboxylase 65 expression level may be involved in the etiology of tinnitus.

Table of Contents

List of Figures and Tables

Chapter 1

Introduction:
Background and Motivation for Research Questions

Critical period plasticity

Plasticity is an ability to change based on experiences. When an organism is born, its brain has yet to learn how to respond to external sound stimuli. Although the basic cortical circuitry is already in place at birth, functional specialization emerges only after experience, through receiving and processing the incoming sensory stimuli. Shortly after birth, organisms undergo a period where their brain is most pliable to change by environmental stimuli. Changes in the brain occurring during this period are long-lasting and usually irreversible, and a similar degree of change cannot be induced once this period has passed. Therefore this period is called the critical period. In my dissertation research, I used rodents as a model organism to study critical period development in the auditory system. In particular, I examined tonotopy—the spatial arrangement of where sound frequencies are processed.

Origin of Tonotopy

The auditory system gives organisms an ability to perceive sound. This ability relies upon auditory sensory organs. Hair cells in the inner ear convert mechanical energy induced by compression of the air into electrical signals. It is the unique mechanical properties of the basilar membrane that separates out different frequency components in the sound and gives rise to the distinct spatial arrangement of sound processing, called tonotopy.

The basilar membrane is an elongated sheet with varying stiffness along its length. The base is stiff and can be activated only by high energy present in high frequency sounds. Therefore, this base preferentially responds to high frequency sound. On the other hand, the floppier tip responds to low-frequency sound. As a result, along the basilar membrane, the represented frequency varies smoothly from high to low in approximately logarithmic manner giving rise to the first instance of tonotopy observed in the auditory pathway.

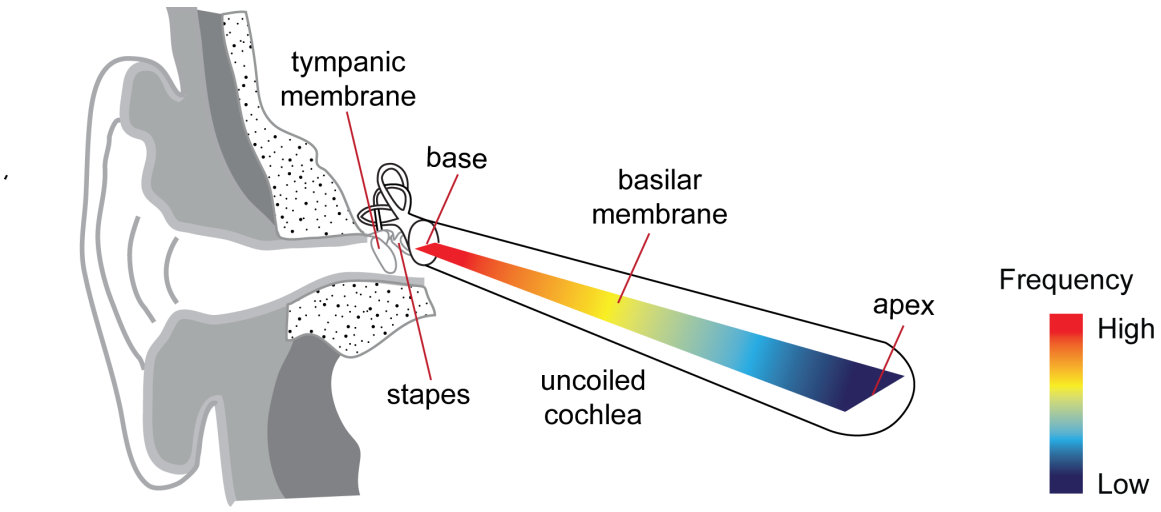

Figure 1.1. Human basilar membrane and its frequency responsiveness (adapted from Kern, Heid et al. 2008)

Following the initial frequency component separation at the basilar membrane, electrical signals are amplified and transmitted via separate bundles of axons, and passed down the auditory pathway. Tonotopic patterns are observed in every auditory brain stem nuclei (Kandler, Clause et al. 2009), as well as in the midbrain (Poon and Chen 1992), thalamus (Barkat, Polley et al. 2011), and primary auditory cortex (Zhang, Bao et al. 2001, De Villers-Sidani, Chang et al. 2007, Han, Köver et al. 2007).

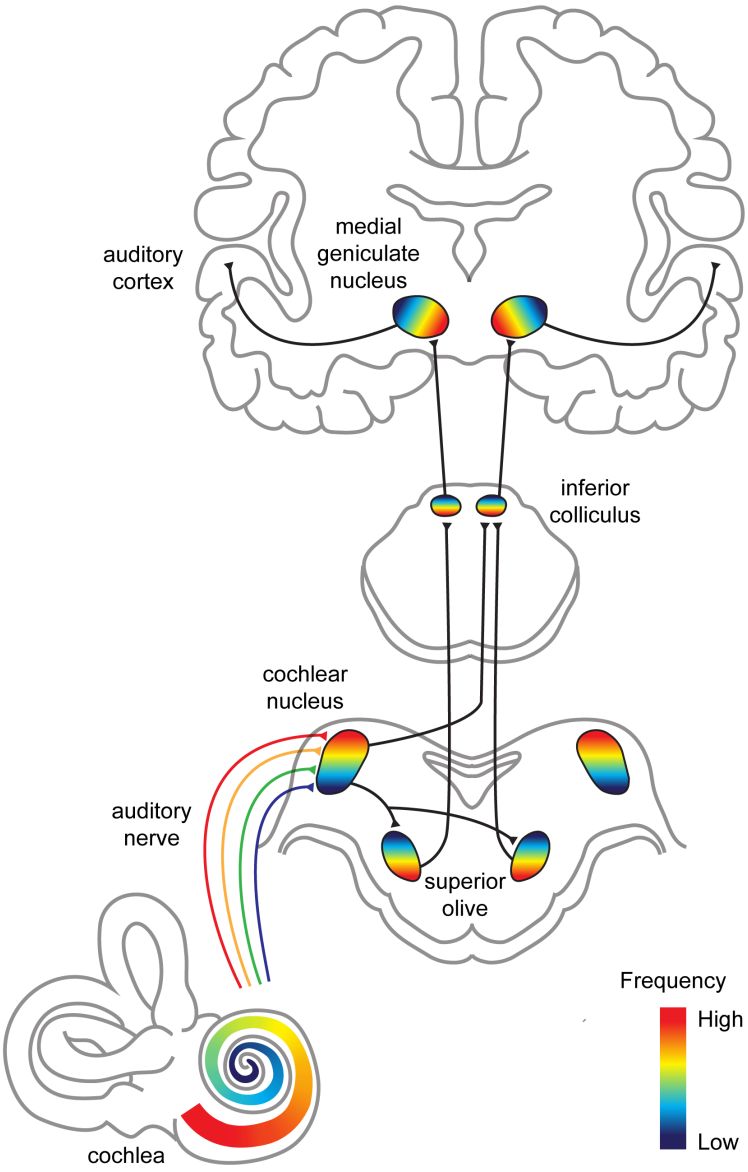

Figure 1.2. Tonotopy of the auditory brainstem circuits (adapted from Kandler, Clause et al. 2009 and Butler and Lomber 2013)

In peripheral parts of the auditory pathway, like the basilar membrane, tonotopy seems to be genetically hard-wired and to be established prior to the onset of hearing (Son, Wu et al. 2012). However, in more central regions, the maturation of tonotopy continues well

into post-natal development, and animals' sensory experiences have a pronounced impact on the tonotopic structure. Many cases of tonotopic plasticity have been reported in AI following manipulation of the acoustic environment in early development (Zhang, Bao et al. 2001, Chang and Merzenich 2003, De Villers-Sidani, Chang et al. 2007, Han, Köver et al. 2007).

Tonotopic Map Plasticity in the Primary Auditory Cortex

In rats, the auditory cortex critical period for pure tones occurs until about day twenty-one after birth (P21). The ear canal opens at around P12, enabling air conduction of sounds. At this point, AI is only responsive to high-amplitude low-frequency sounds, which presumably can be transmitted via bone conduction (De Villers-Sidani, Chang et al. (2007). After ear canal opening, the range of frequency representation expands rapidly between P11 and P14. By P21, spectral tonotopy and other response properties of AI neurons appear equivalent to those recorded in adult rats (De Villers-Sidani, Chang et al. 2007).

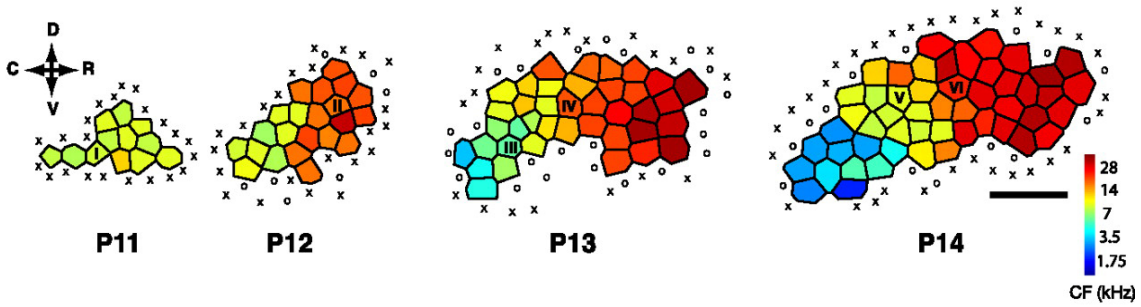

Figure 1.3. Development to AI tonotopy from postnatal day 11 to 14 (De Villers-Sidani, Chang et al. 2007)

Previous studies have documented effects of acoustic manipulation during the auditory critical period. For instance, repeated exposure to single frequency tone pips induces an enlarged representation of that tone in AI (Zhang, Bao et al. 2001, De Villers-Sidani, Chang et al. 2007) and has lasting effects in perception and sound-guided behavior (Han, Köver et al. 2007).

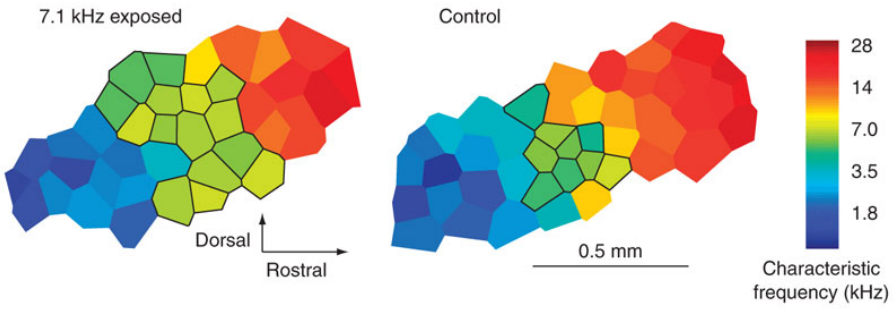

Figure 1.4. Expansion of sound exposure frequency following 7.1 kHz pure-tone rearing (Han, Köver et al. 2007)

While the effects of tone rearing in AI are well characterized, the original locus of this tonotopic change remained unclear. Tonotopy is observed not just in AI but also in upstream auditory nuclei. Could the tonotopic changes observed in AI arise from a feed-forward manifestation of tonotopic changes upstream of the auditory cortex? In Chapter 2, I explore this question by contrasting the tonotopy of AI and inferior colliculus in juvenile rats that underwent tone rearing.

Hearing Loss and Acoustic Perceptual Disorder

Plasticity is not limited during the development and occurs throughout life. One form of adult plasticity occurs following damage to sensory organs or nerves. This type of plasticity is well documented in the somatosensory domain, following a digit amputation in primates (Merzenich, Nelson et al. 1984), or trimming of whiskers in rodents (Van der Loos and Woolsey 1973). Following the loss of inputs from a peripheral sensory organ, the spatial representation in the cortex, or topographic map, undergoes change. The part of the topographic map that previously represented the damaged body part shrinks and neighboring representation appear to take over.

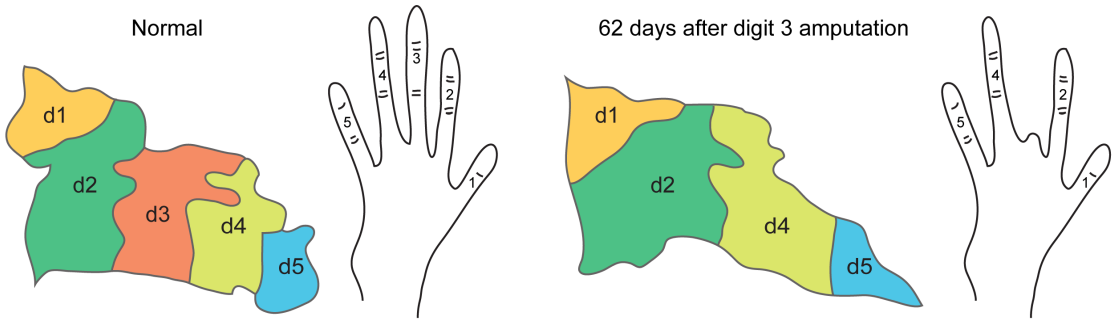

Figure 1.5. Somatosensory cortex topographical map reorganization after finger amputation (adapted from Merzenich, Nelson et al. 1984)

The perceptual implication of such topographical change is unclear—yet it has been hypothesized to be an underlining cause of peculiar perceptual disorders like phantom limb syndrome (Ramachandran and Rogers-Ramachandran 2000).

Similar changes in spatial representation have been observed in AI tonotopy following hearing loss due to damage to hair cells. The hair cell is a delicate organ and can be permanently damaged by exposure to loud sound. Following frequency-specific sensorineural damage, AI tonotopy reorganizes itself so that the damaged area is taken over by neighboring undamaged frequencies (Eggermont and Roberts 2004, Noreña and Eggermont 2005). This change of tonotopy has been hypothesized to underlie perception of phantom sound, or tinnitus. In Chapter 3, I investigated whether tonotopic reorganization is an underlining cause of tinnitus.

Chapter 2

Plasticity of Tonotopic Representation in the Developing Auditory Cortex and Inferior Colliculus

Asako Miyakawa, Robert Gibboni, and Shaowen Bao

Originally published in *Neuroscience*

January 29, 2013

Abstract

Early acoustic experience changes tonal frequency tuning in inferior colliculus (IC) and primary auditory cortex. The contributions of IC plasticity to cortical frequency map reorganization are not entirely clear. While most cortical plasticity studies exposed animals to pulsed tones, studies of IC plasticity used either noise or a continuous tone. Here we compared the effects of repeated exposure to single-frequency tone pips on cortical and IC frequency representations in juvenile rats. We found that while tone exposure caused a long-lasting increase in cortical representations of the exposure frequency, changes to IC neurons were limited to a transient narrowing of tuning bandwidth. These results suggest that previously documented cortical frequency map reorganization does not depend on similar changes in subcortical auditory nuclei.

Introduction

Early acoustic experience can lead to long lasting changes in neural response properties (Sanes and Constantine-Paton 1985, Zhang, Bao et al. 2001, Chang and Merzenich 2003, de Villers-Sidani, Chang et al. 2007, Han, Kover et al. 2007, Insanally, Kover et al. 2009, Kim and Bao 2009, Barkat, Polley et al. 2011). Previously, we demonstrated that exposing a rat to 7-kHz pure tone during the auditory critical period increased the number of neurons tuned to 7 kHz in primary auditory cortex (AI). This developmental plasticity has lasting effects on the animal's sensory perception and behavior (Han, Kover et al. 2007). Auditory cortex reflects the statistics of environmental sounds by modifying its sound representation, or the tonotopic map. However, we know surprisingly little about the original locus or loci of tonotopic map plasticity. In theory, altered frequency tuning observed in the auditory cortex could arise from a feed-forward manifestation of synaptic changes upstream of the auditory cortex, such as auditory brain stem nuclei (Sanes and Constantine-Paton 1985, Poon and Chen 1992, Yu, Sanes et al. 2007). Should that be the case, molecular and cellular studies of auditory plasticity should focus first on subcortical auditory structures before studying downstream effects in the cortex.

Currently, limited reports are available on whether subcortical structures show AI-like reorganization of tonotopic map following manipulation of early acoustic experience. One study reported AI-like tonotopic changes in the central nucleus of inferior colliculus (ICC) following exposure to single continuous tone (Poon and Chen 1992). Tuning bandwidth and other response properties of ICC neurons can also be changed by exposure to clicks and noises (Sanes and Constantine-Paton 1983, Sanes and Constantine-Paton 1985, Grecova, Bures et al. 2009, Bures, Grecova et al. 2010) or paired pure tones (Yu, Sanes et al. 2007). Oliver and colleagues examined ICC frequency map following repeated tone exposures that were similar to those used in early cortical plasticity studies (Oliver, Izquierdo et al. 2011). However, their methods of response analysis were different from those of the cortical studies, hindering a direct comparison with parallel cortical plasticity effects (see Discussion for details). In order to address this issue, we studied tonotopic organizations of both ICC and AI in rat pups reared in an acoustic environment of repetitive tone pips, which has been previously shown to induce a change in cortical tonotopic organization (Han, Kover et al. 2007).

Results

The total number of animals, their mean ages and the numbers of multiunits are reported in Table 1. The peak latency, firing threshold and peak response firing rate of the multiunits were not different between sound exposed animals and their age matched controls (Table 2.1).

ICC tonotopic representation is not altered following acoustic exposure.

CFs of ICC multiunits were plotted as a function of dorso-ventral recording depth relative to the most dorsal ICC site. ICC exhibits smooth tonotopy from low to high CF dorso-ventrally, covering roughly 4 octaves over 1500 μm. Overrepresentation of the exposure

frequency was expected to manifest as an increased number of units tuned to 7.5 kHz ± 0.2 octaves. However, no differences were observed in the proportion of sites tuned to the exposure frequency when comparing between control and experimental groups for both Early and Late mapping windows (Fig 2.1).

ICC multi-unit tuning bandwidth changes as a result of acoustic exposure.

Tuning curve bandwidth (BW), the frequency range to which a multiunit responds, was measured at 30dB above multiunits' firing threshold (BW30) and compared between control animals and exposed animals mapped during the Early and Late mapping windows. Statistical analysis did not show any significant difference, possibly because tuning bandwidth varied substantially between animals. To identify potential frequency-specific effects, we normalized the BW30 within each animal and compared their Z-scores. Animals in the Early mapping group showed a significant narrowing of BW for sites tuned to the exposure frequency (one-tailed two sample t-test at 7.5kHz ± 0.2 octave: $p = 0.0095$) (Fig 2.3a). No BW effects were observed when ICC was mapped in the Late mapping window (Fig 2.3b).

AI tonotopic representation changes following acoustic exposure.

AI tonotopy was examined in the littermates that underwent the same acoustic rearing as the ICC animals. AI tonotopic axis, defined here as the straight line connecting the site of the lowest and highest CF in AI tonotopy, showed a clustering of units tuned around 7.5 kHz (Figure 2.4a). Acoustic rearing induced an enlargement of the cortical area tuned to the exposure frequency in AI (Fig 2.4b: one-tailed two sample t-test at 7.5kHz ± 0.2 octave: $p=0.0062$), consistent with previous studies (Zhang, Tao et al. 1998, de Villers-Sidani, Chang et al. 2007, Han, Kover et al. 2007, Kim and Bao 2009).

Bandwidths of AI frequency-intensity areas were examined at 30 dB above firing threshold. To be consistent with the ICC bandwidth analysis, we also Z-scored the BW30 for cortical responses. No differences were observed between sound-exposed and control animals (Fig 2.4c).

Discussion

Few studies have compared tonotopic map changes in both auditory cortex and inferior colliculus using exactly the same rearing paradigms. Here, we show that tonotopic map changes induced by pure tone acoustic rearing are limited to AI and absent in ICC under our experimental conditions. We conclude that tonotopic reorganization in AI following acoustic rearing does not depend on similar changes in ICC. This is consistent with previous findings that conductive hearing loss-induced tonotopic map plasticity occurs in AI but not in ICC (Popescu and Polley 2010).

Further, we have demonstrated a reduction of receptive field bandwidth in ICC multiunits with characteristic frequencies around the acoustic exposure. Notably, this bandwidth effect was only present in our Early mapping groups (P17-24), and not in the Late mapping groups (P40-51), despite the identical acoustic exposure during the auditory

critical period. These results suggest that the ICC bandwidth effects are transient, while AI tonotopic map change is persistent well after (>15days) the termination of acoustic rearing. Equivalent bandwidth effects were absent in AI in the present study. A previous study reported reduced tuning bandwidth after pure tone exposure in AI multiunits tuned to the exposure frequency (Han, Kover et al. 2007). The discrepancy may be due to differences in experimental procedures and methods of data analysis—in the previous report, animals had gone through behavioral tests before their AI were mapped, and the tuning bandwidth were derived from rate-frequency tuning curve instead of intensity-frequency tuning curve.

Suga and colleagues extensively documented a similar distinction between experience-induced tuning changes in IC and AI in the bat. For example, fear conditioning results in frequency tuning shifts for both cortical and ICC neurons, with changes in ICC neurons occurring earlier, but decaying much faster, than in cortical neurons, suggesting that transient ICC plasticity may contribute to long-term cortical reorganization (Gao and Suga 1998, Gao and Suga 2000). In those studies, plasticity was induced in adult animals using either electrical stimulation or behavioral conditioning. In the present study, we observed transient bandwidth change in the ICC immediately after tone exposure, but did not observe any tuning shifts in the ICC. It appears that, in both bats and rats, ICC exhibits transient experience-dependent spectral plasticity, whereas AI shows long-lasting reorganization of the frequency map.

Developmental plasticity in frequency tuning has been previously reported in the ICC. When mice were exposed to repetitive clicks, a stimulus that co-activates afferents across a broad frequency range, single ICC neurons became more broadly tuned to frequency (Sanes and Constantine-Paton 1983, Sanes and Constantine-Paton 1985, Grecova, Bures et al. 2009, Bures, Grecova et al. 2010). Broadening of the ICC tuning bandwidths has also been reported in adult rats that were exposed to a 125 dB broadband noise for eight minutes at postnatal day 14 (Grecova et al., 2009, Bures et al, 2010). Similarly, when animals were exposed to two simultaneously played tones, ICC neurons became broadly tuned (Yu, Sanes et al. 2007). Their primary bandwidth finding is in general agreement with our results. Taken together, these findings suggest that ICC neurons exhibit bidirectional bandwidth plasticity, narrowing or broadening depending on the stimuli. The discrepancy between results of the present study and those of Poon et al (Poon and Chen 1992) may be due to differences in the sound exposure and unit sampling procedures.

Oliver and colleagues (Oliver, Izquierdo et al. 2011) exposed juvenile rats to repetitive tone pips using stimulus parameters and exposure time windows that were similar to those of our study and previous studies of auditory cortical plasticity (Zhang, Bao et al. 2001, de Villers-Sidani, Chang et al. 2007). They reported that more ICC sites were tuned to the exposure frequency after the animals were repeatedly exposed to a 14-kHz tone using the stimulus parameters of Zhang and colleagues (Zhang, Bao et al. 2001). However, they did not report consistent tonotopic effects in animals that were exposed to a 7-kHz tone following the stimulus parameters of the de Villers-Sidani and colleagues (de Villers-Sidani, Chang et al. 2007). After both exposure conditions, subsets of ICC

neurons showed reduced responses to the exposure frequency (Oliver, Izquierdo et al. 2011). The discrepancy between our results and those of Oliver and colleagues may be due to differences in animal strains (SD vs. Long Evens), recording electrodes (multi-site silicon probe vs. tungsten-in-glass), CF identification methods (off-line scoring by "blind" experimenters vs. on-line searching with the help of an oscilloscope and audio monitor), frequency scales (logarithmic vs. linear) and quantification of representational sizes (fixed CF bins vs. variable CF steps).

A negative finding of ICC tonotopic reorganization might be attributed to several confounding factors. For instance, the acoustic exposure length might have been too short for some animals in the Early mapping group, since the exposure was terminated by the ICC mapping. Since the rat ear canal opens at approximately P12, the shortest exposure length used in our study was ~5 days. AI tonotopic map changes can be induced by acoustic exposure for as short as 3 days (de Villers-Sidani, Chang et al. 2007). Another confounding possibility is that ICC undergoes a very brief transient tonotopic reorganization, which was not captured in our mapping interval. We mapped at a range of ages within the Early mapping group to maximize the chance of capturing such transient effects. Although our experimental design cannot completely rule out the possibility of transient ICC map changes, our results suggest that persistent changes in ICC are not required for the long-lasting AI map reorganization. Finally, ICC tonotopic reorganization might not be expressed under urethane anesthesia. Again, the fact that we were able to observe map changes in AI but not in ICC under identical anesthetic procedures suggests that the cortical map reorganization does not depend on an expression of associated map changes in ICC, if any.

Afferent fibers from ICC synapse at medial geniculate nucleus (MGN) of thalamus before reaching AI. Although we did not investigate plasticity of MGN, our ICC bandwidth finding is in line with a report on thalamocortical plasticity (Barkat, Polley et al. 2011). In that study, Barkat et al. exposed juvenile mice to repeated pure tone pips and contrasted the tonotopic organization at thalamus and AI. In the MGN, this manipulation led to a narrowing of bandwidth at the exposure frequency without changing the tonotopic representation, while the AI tonotopic map showed overrepresentation at the exposure frequency. Given these findings, it appears that robust tonotopic reorganization following repeated sound exposure is a reserved property of the cortex, and that this effect is not a simple readout from upstream subcortical auditory nuclei.

Efforts to identify the source of auditory plasticity is significantly complicated by the existence of extensive feedback projections from auditory cortex to ICC and other nuclei of the inferior colliculus (Saldana, Feliciano et al. 1996). There is compelling evidence that auditory cortex modulates spectral selectivity of lower auditory nuclei via feedback projections (Yan and Suga 1996, Zhang, Suga et al. 1997). Moreover, stimulation of ICC neurons was found to cause a shift of the frequency tuning in nearby ICC neurons. This shift was abolished by cortical inactivation, suggesting that ICC stimulation must go through the cortex in order to produce effects on ICC itself (Zhang and Suga 2005). Selective manipulation of auditory pathways using newer techniques (e.g. optogenetic) will reveal the exact nature of subcortical contributions to cortical tonotopic map

reorganization and will help us gain further insight into the mechanisms of auditory pathway plasticity.

Methods

Sound exposure

All procedures used in this study were approved by the University of California Berkeley Animal Care and Use Committee. A litter of rat pups and dam (Sprague Dawley) was placed in an anechoic sound-attenuation chamber, and trains of pure tone pips (7.5 kHz, 60 dB SPL, 100-ms pip duration, 5-ms cosine squared ramp, six pips in a train at 6 Hz, one train every 2 s) were played 24 hours a day to the animals during a period from postnatal day 9 (P9) to P25 (Fig 2.1). This time window covers the critical period for spectral representation plasticity in the primary auditory cortex (AI) and has been used in previous studies (Insanally, Kover et al. 2009). After sound exposure, animals were returned to standard housing conditions. A control litter was maintained in the standard animal husbandry room.

AI mapping

The AI of sound-exposed and control animals were mapped at comparable ages between P37 to P96 (exposed, n = 4, mean P67.50, SD 20.04, naïve, n= 4, mean P52.75 SD 11.15). Rats were anesthetized with urethane (2.0 g/kg, i.p.). Atropine sulfate (0.1 mg/kg, s.q.) and dexamethasone (1 mg/kg, s.q.) were administered to reduce brain edema and viscosity of bronchial secretions. The anesthetized rat was placed in a custom head holder and a slit was made in the cisterna magna to drain cerebrospinal fluid and reduce brain pulsations. A craniotomy and durectomy was performed over right AI. A layer of silicon oil was applied to prevent brain desiccation. Sound stimuli were generated by an audio signal processor (Tucker-Davis Technologies RX6) and delivered to the left ear from an enclosed cannulated speaker (Tucker-Davis Technologies Electrostatic Speaker, Coupler model) through a tube. The speaker was calibrated to have <3% harmonic distortion and flat output in the entire frequency range (Tucker-Davis Technologies SigCal32).

Multiunit responses of AI neurons were recorded using tungsten microelectrodes (FHC) advanced orthogonally to the cortical surface to the cortical layer IV (450-600μm). Electrical signals were amplified and recorded for 333ms surrounding each stimulus presentation (Tucker-Davis Technologies RX5). Prior to each recording block, search stimuli (white noise bursts, 60dB SPL, 25ms duration, repeated at 3Hz) were played to identify sound-evoked multiunit responses. Multiunit responses were defined as voltage changes that exceed the mean amplitude of the baseline electrical trace by two standard deviations. Thresholds for multiunit discrimination were set for each microelectrode before recordings. Pure tone pips of 51 frequencies (1-32 kHz, 0.1 octave spacing, 5-ms cosine-squared ramps, 25-ms duration, repeated three times) at 8 intensities (0-70 dB SPL, 10 dB spacing) were presented in pseudorandom order, and responses were used to reconstruct the frequency-intensity receptive field of each multiunit.

Electrode penetrations were made densely throughout the temporal cortex while avoiding surface blood vessels. On average, 71 penetrations (SD ±14) were made in the area of AI (mean area 2.41 ± 0.44mm^2), corresponding to roughly 215µm between penetrations. Recording sites were marked on a magnified digital photograph of the cortex for later tonotopic map reconstruction.

ICC mapping

The inferior colliculus of 7.5 kHz-experienced and naïve rats was mapped at comparable ages in two time windows: an Early mapping window at the end of the acoustic exposure between P17 and P24 (exposed, n = 4, mean age P19.25 ± 2.22, naïve, n = 3, mean age P18.33 ± 5.51), and a Late mapping window at least 15 days after the acoustic exposure, between P40 and P51 (exposed, n = 7, mean age P45.1 ± 3.44, naïve, n= 3, mean age P47 ± 2.65). Anesthetics, surgical procedures and the speaker setup were identical to those used in the AI mapping.

Multiunit recording was made from the right inferior colliculus. A burr hole was made on the skull stereotaxically 1mm lateral and 1mm rostral to lambda. A 16-channel polytrode (NeuroNexus Technologies; 1 shank, 50 µm contact spacing, 177 µm^2 contact site, model A1x16-3mm-50-177; or 4 shanks, 125 µm shank spacing, 50µm contact spacing on each shank, 177µm^2 contact site, model A4x4-3mm-50-125-177) was lowered vertically into the inferior colliculus while search stimuli were being played, until strong auditory evoked responses were observed. Penetrations were made at multiple locations of IC and the central nucleus of IC (ICC) was differentiated from other IC nuclei by its tonotopic organization and sharp frequency-intensity tuning. Only ICC multiunits were included in the analysis. Regular spacing of recording sites on each shank of the polytrode ensured unbiased sampling from the ICC. The polytrode was advanced in set distance intervals (50 µm for 4-shank, or 200 µm for 1-shank polytrode) in a single track to record the entire dorsal-ventral extent of ICC. Undersampling of units at the beginning and the end of each electrode track was accounted for during the data analysis.

Frequency-intensity tuning curve of each multiunit was reconstructed from its responses to 25ms pure tone pips of 51 frequencies (1-32 kHz, 0.1 octave spacing, repeated three times) and 8 sound pressure levels (0 – 70 dB SPL, 10 dB steps). The tonotopic axis was defined as the dorso-ventral recording site depth relative to the most dorsal ICC site encountered. Tonotopy of ICC was compared between the 7.5 kHz-experienced and naïve animals to examine the effect of tone rearing on spectral representations.

Data analysis

Off-line data analysis and statistical tests were conducted using MATLAB (MathWorks). The characteristic frequency (CF) of auditory cortical and ICC multiunits was determined as the frequency at which the lowest intensity sound evokes a neural response. CF and tuning bandwidth at 30dB above multiunits' firing threshold (BW30) were determined visually from the V-shaped response-frequency curve by experienced experimenters blind to the acoustic exposure conditions. Peak latency was defined as the poststimulus

duration to the peak of the peristimulus time histogram. Peak firing rate was defined as the spike rate during the 2-ms surrounding this peak.

Since pure tone exposure has been associated with overrepresentation and an accompanying decrease in tuning bandwidth at the exposure frequency (Poon and Chen 1992, Zhang, Tao et al. 1998, Han, Kover et al. 2007, Barkat, Polley et al. 2011), we hypothesized that similar frequency-specific effects would be observed in the present study. Therefore, we performed one-tailed t-tests on tonotopic frequency representation and tuning bandwidth at the exposure frequency (7.5 kHz ±0.2 octave) to determine the statistical significance of differences between sound-exposed and control groups.

Appendix 2: Figures

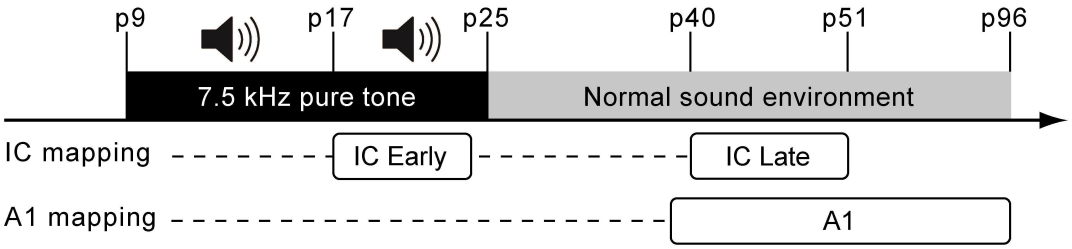

Figure 2.1. Timeline of the experiments

Rats were exposed to 7.5-kHz pure tone pips between P9 and P25. Recordings were made from the inferior colliculus (IC) in an Early (P17 – P24) or Late (P40 – P51) mapping window. All AI mappings were performed in P36 – P96 rats.

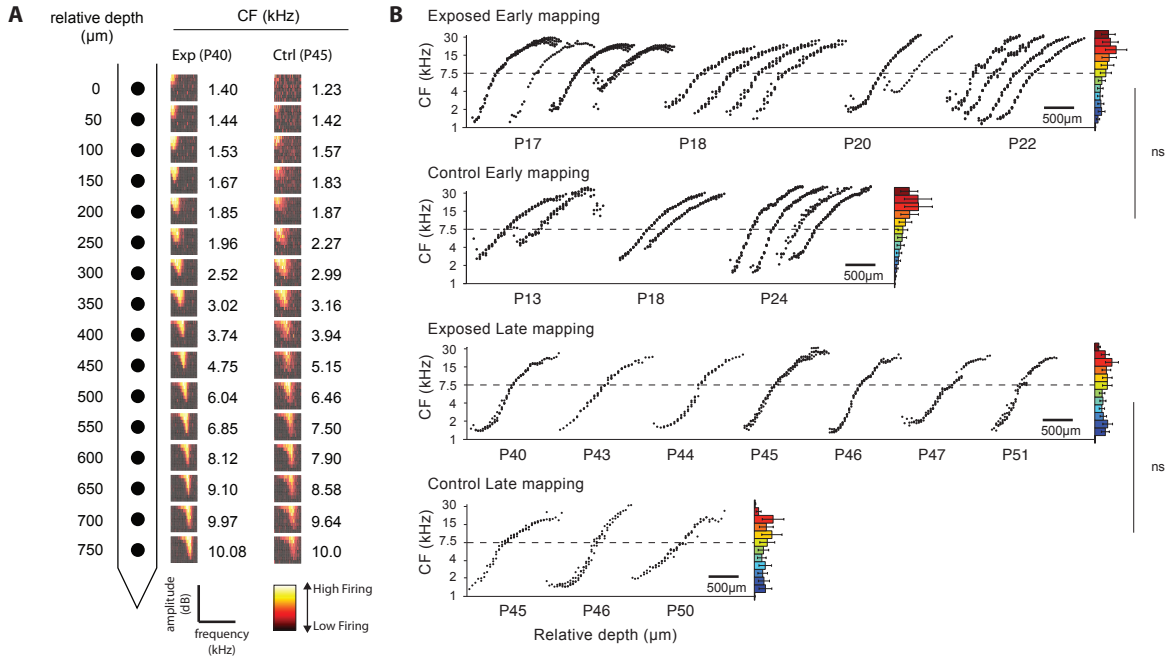

Figure 2.2. ICC tonotopic representation following acoustic exposure

A. Sample receptive fields from two animals using 1 shank 16 channel polytrode. Receptive fields are plotted based on multiunits' responses to each frequency (x-axis: 1-32 kHz, 0.1 octave spacing) and amplitude (y-axis: 0-70 dB SPL, 10 dB spacing) combination. Colorbar is scaled to the maximum firing in each panel. **B**. The characteristic frequencies (CFs) for each IC site are plotted as a function of recording depth (scale shown at right). Multiple recording tracks are shown for some animals. To the right, histograms indicate the proportion of sites with CFs at the corresponding frequency. For all figures, error bars indicate standard error of the mean (SEM). The proportion of sites tuned near the exposure frequency (7.5 kHz ± 0.2 oct) for exposed and control animals did not differ significantly for recordings made during both the Early and Late windows.

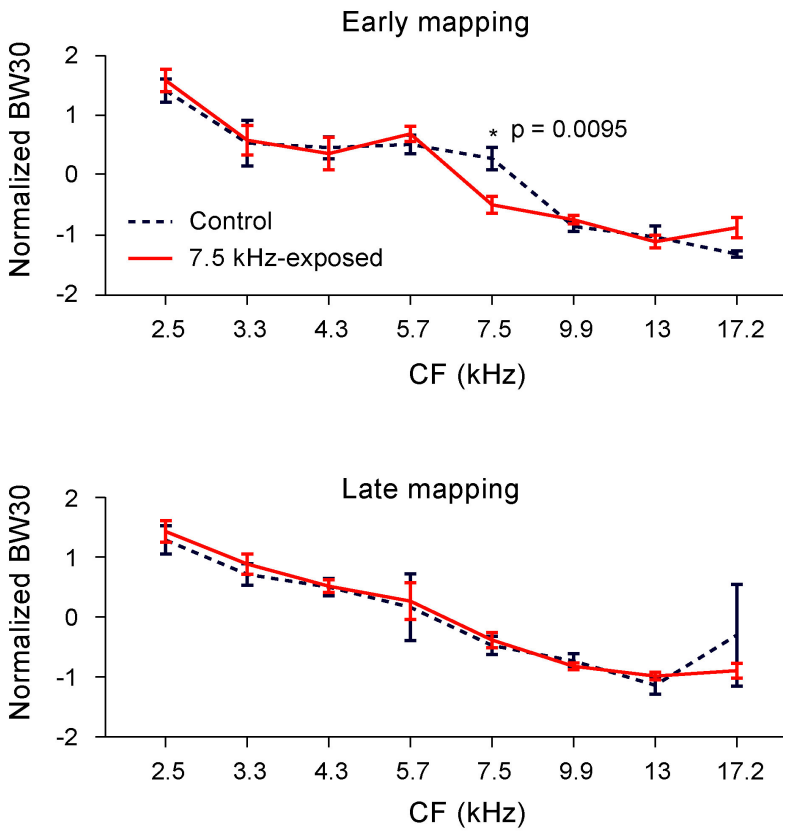

Figure 2.3. ICC bandwidth following acoustic exposure

Tuning bandwidth of IC sites measured 30 dB above firing threshold is plotted as a function of that site's characteristic frequency (CF) for control (blue) and exposed (red) animals. In exposed animals mapped in the Early window, a significant reduction in tuning bandwidth was observed for sites tuned near the exposure frequency. No differences were observed in the Late mapping window.

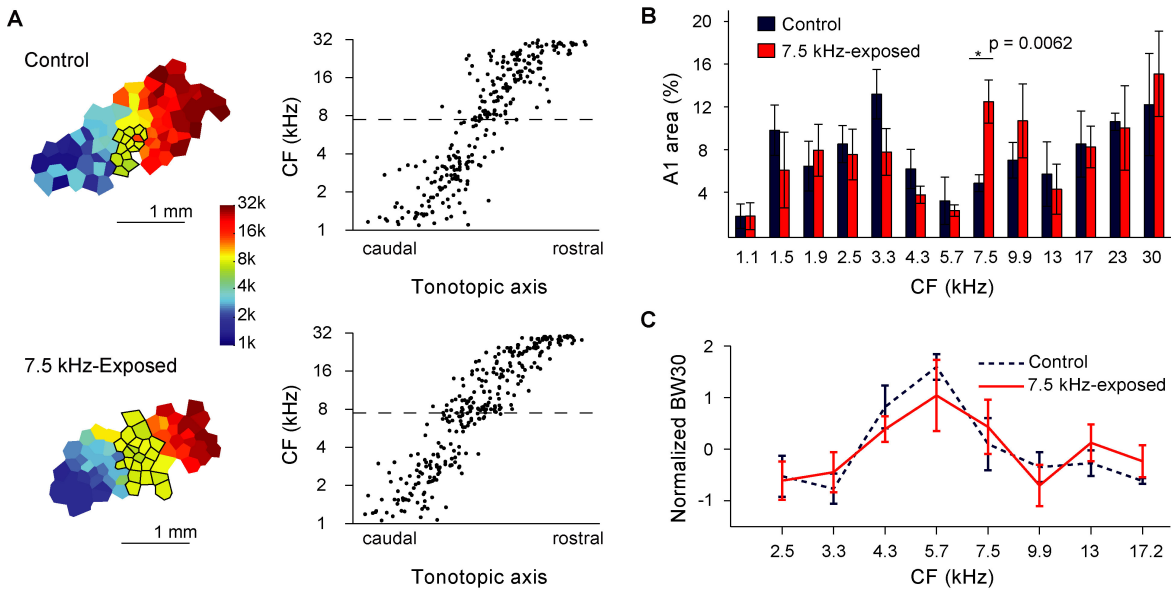

Figure 2.4. AI tonotopic representation following acoustic exposure

A. representative tonotopic maps recorded from primary auditory cortex (AI) are shown. Polygons were generated using Voronoi 18pprox.18tion of all AI recording sites. Warm and cool colors indicate sites tuned to high and low frequencies, respectively. Right: scatterplots showing characteristic frequency (CF) of each site as a function of its location along the tonotopic axis. **B**. A histogram showing the proportion of each map tuned to different frequency bands in control (blue) and exposed (red) animals. In exposed animals, significantly more of AI is tuned to the exposed frequency. **C**. Average bandwidths 30 dB above firing threshold (BW30) are displayed as a function of characteristic frequency (CF). No differences are present between control and exposed animals

Table 2.1. Basic response properties of ICC and AI multiunits

	ICC Early mapping window (P17-P24)			ICC Late mapping window (P40-P51)			AI mapping (P37-P96)		
	control	exposed	p-value	control	exposed	p-value	control	exposed	p-value
n	3	4		3	7		4	4	
age (days)	18.33±3.89	19.25±1.28	0.78	47.00±1.87	45.14±1.40	0.43	52.75±6.44	67.50±11.57	0.25
multiunits (per animal)	370.67±155.78	458.00±100.30	0.58	85.33±6.53	182.86±88.75	0.47	67.50±10.80	73.75±5.46	0.57
Peak Latency (ms)	17.32±1.33	21.74±1.92	0.10	14.32±0.45	15.19±1.22	0.64	23.97±3.06	20.72±1.05	0.29
Firing threshold (dB SPL)	33.25±3.57	31.11±1.61	0.50	22.44±7.10	27.14±2.20	0.35	29.01±4.26	32.39±2.14	0.44
peak FR (Hz)	43.25±8.66	37.09±12.90	0.69	85.69±10.66	73.76±12.72	0.55	34.47±3.14	38.78±5.33	0.45

Data are presented as means ± SEM. P-values are reported from two-sample t-tests conducted between control and exposed animals.

Chapter 3

Plasticity in the adult auditory cortex following hearing loss

Abstract

Hearing loss is the biggest risk factor for tinnitus and hearing loss-related pathological changes in the auditory pathway have been hypothesized as the mechanism underlying tinnitus. However, due to the comorbidity of tinnitus and hearing loss, it has been difficult to differentiate between neural correlates of tinnitus and consequences of hearing loss. In this study, we dissociated tinnitus and hearing loss in FVB mice, which exhibit robust resistance to tinnitus following noise-induced hearing loss. Furthermore, knockdown of glutamate decarboxylase 65 (GAD65) expression in auditory cortex by RNA interference gave rise to tinnitus in normal-hearing FVB mice. We found that tinnitus was correlated with down-regulation of GAD65 in the auditory cortex. By contrast, cortical map distortions, which have been hypothesized as a mechanism underlying tinnitus, were correlated with hearing loss but not tinnitus. Our findings suggest new strategies for the rehabilitation of tinnitus and other phantom sensation, such as phantom pain.

Introduction

Tinnitus is the phantom perception of sounds in the absence of corresponding external sound. Its clinical etiology is diverse, including hearing loss, ototoxic drugs, ear infection, vascular abnormality and tumors(Henry, Dennis et al. 2005, Langguth, Kreuzer et al. 2013). Among these, the biggest risk factor is hearing loss due to aging or acoustic trauma(Salvi, Wang et al. 2000, Eggermont and Roberts 2004, Heffner and Koay 2005, Henry, Dennis et al. 2005, Elgoyhen and Langguth 2010). However, despite high comorbidity, hearing loss does not always lead to tinnitus. People can have significant hearing loss and still do not develop tinnitus or vice versa(Lockwood, Salvi et al. 2002, Møller 2011). Indeed, the prevalence of hearing loss is much higher than that of tinnitus(Lockwood, Salvi et al. 2002), and the two follow different aging trajectories(Møller 2011). It is likely that the development of tinnitus involves complex interactions between an individual's health conditions (hearing and otherwise) and genetic predispositions(Sand, Langguth et al. 2007). Recent studies using mouse models showed that noise-induced tinnitus can be observed in multiple commonly used laboratory mice strains(Longenecker and Galazyuk 2011, Middleton, Kiritani et al. 2011, Llano, Turner et al. 2012). Previous studies have also revealed cross-strain differences in tinnitus etiology with respect to age-related hearing loss(Zheng, Johnson et al. 1999, Turner, Brozoski et al. 2006) and vulnerability to acoustic injury(Davis, Cheever et al. 1999). Systematic comparisons of tinnitus in different strains of mice may inform neural correlates of individual differences in tinnitus susceptibility in humans. In addition, such comparisons may provide insights into the neural mechanisms underlying tinnitus.

Loss of hearing leads to reduced sensory input and lower auditory nerve discharge rates (Liberman and Kiang 1978), which should decrease neuronal activity levels in the central auditory system. Paradoxically, spontaneous neuronal activity is elevated along the auditory pathway in animal models of noise trauma-induced tinnitus (Norena and Eggermont 2003, Wang, Brozoski et al. 2011). This increase in spontaneous activity could be caused by imbalanced excitation and inhibition, either from enhancement of neuronal excitation, reduction in inhibition or altered neuronal excitability as a result of hearing loss (Kotak, Fujisawa et al. 2005, Schaette and Kempter 2006, Sun, Zhang et al. 2008, Middleton, Kiritani et al. 2011, Yang, Weiner et al. 2011, Llano, Turner et al. 2012). In addition, noise exposure causes distortion of the cortical frequency map (Engineer, Riley et al. 2011) and changes neuronal discharge patterns (e.g. increased synchrony and more burst firing) (Norena and Eggermont 2003, Seki and Eggermont 2003, Engineer, Riley et al. 2011, Kaltenbach 2011). All these noise-induced neurophysiological changes have been considered to be potential mechanisms of tinnitus.

A challenge in tinnitus research is that it is difficult to dissociate the mechanisms underlying tinnitus from the effects of hearing loss. For example, behavioral tests of tinnitus in animal models, including both the gap detection(Turner, Brozoski et al. 2006) and conditioning-based methods(Bauer and Brozoski 2001, Lobarinas, Sun et al. 2004), rely on the animal's hearing ability. Therefore, measurements of tinnitus could be confounded by hearing loss. In addition, dissociation of tinnitus from hearing loss is difficult because tinnitus severity can correlate with the degree of hearing loss (Tan,

Ruttiger et al. 2007). Even in noise-exposed animals that have apparently recovered normal auditory brainstem response (ABR) thresholds, careful analysis has revealed substantial loss of cochlear neurons and reduction in neuronal response amplitude(Kujawa and Liberman 2009). Thus, the observed electrophysiological changes in animals with noise-induced tinnitus could be due to hearing loss rather than tinnitus. To fully distinguish the neural mechanisms of tinnitus from the neurophysiological changes caused by hearing loss, tinnitus needs to be completely dissociated from hearing loss.

Here, we found that noise-induced hearing loss (NIHL) resulted in *behavioral evidence of tinnitus* (hereafter referred to as *tinnitus*) in C57BL/6 and Tg(dlx6a-cre)1Mekk mice, but not FVB mice. By contrast, knockdown of cortical GAD65 expression by virus-mediated RNA interference resulted in tinnitus in normal hearing mice as measured with two behavioral tests—gap detection and conditioned active avoidance. This double dissociation allowed us to isolate the neural correlates of tinnitus from the electrophysiological consequences of hearing loss. We report that downregulation of cortical GAD65 expression is correlated with tinnitus, whereas cortical map reorganization is correlated with hearing loss.

Results

Strain difference in hearing loss-induced tinnitus

To assess whether hearing loss results in tinnitus, we administered NIHL in the left ear of mice using 112dB 8 kHz-centered noise for 2 hours and tested gap detection behavior (Fig 3.1a) before and after NIHL. Two strains of mice—FVB and C57BL/6—were used for this NIHL experiment. A supporting experiment, described below, shows consistent results using Tg(dlx6a-cre)1Mekk mice. See Fig 3S.1 for the summary and timeline of all experiments.

Noise exposure resulted in significant and persistent ABR threshold shifts for the exposed (left) ear in both C57BL/6 (n = 8) and FVB (n = 8) (ANOVA, session, $F_{1,14} = 374.64$, $p < 0.001$, paired sample t-test, $p < 0.05$ for 4-32 kHz, Fig 3.1b-c top). This ABR threshold shift was maintained for at least 20 days after NIHL. The magnitudes of the ABR threshold shifts were similar between the two strains (ANOVA, strain-by-session interaction, $F_{1,14} = 1.02$, $p = 0.33$). In both strains, the untreated (right) ear maintained pre-exposure threshold (Fig 3.1b-c top), peak latency, and peak amplitude (Fig 3S.2), indicating a successful unilateral NIHL.

Tinnitus was measured by the impairment it causes in detecting a gap in a constant background sound (Turner, Brozoski et al. 2006, Fournier and Hebert). Gap detection was quantified by the ratio of cued-over-uncued average startle amplitudes, with a lower ratio indicating better gap detection. Gap detection was examined in three sessions—pre-NIHL, and 2 days and 10 days post-NIHL—in FVB (n=10) and C57BL/6 mice (n=8, Fig 3.1b-c bottom). Before NIHL, FVB exhibited higher raw startle amplitude than C57BL/6 for both cued and uncued trials ($p < 0.05$ for all frequencies for uncued, 2 out of 5

frequencies for cued, unpaired t-test). However, there was no strain difference in gap detection performance as measured by startle response ratio (i.e. cued-over-uncued average startle amplitudes ratio) for any carrier tone frequency (ANOVA, strain-by-frequency interaction, $F_{4,14} = 1.93$, $p = 0.16$). After NIHL, we observed a general reduction in raw startle amplitude in both strains ($p < 0.05$ for all frequencies, paired t-test). The percentage reduction of uncued raw startle amplitude was similar between the two strains (ANOVA, session-by-strain interaction, $F_{1,16} = 0.07$, $p = 0.80$). Reduction of acoustic startle reflex after NIHL has previously been reported, and raised a concern that it could bias for a higher startle response ratio in gap detection(Lobarinas, Hayes et al. 2013). However, there was no correlation between raw startle amplitude and the startle response ratio in our study (Pearson correlation between average uncued startle amplitude and associated startle response ratio. $R = 0.04$, $n = 180$, $p = 0.64$. Data pooled from all subjects and test sessions).

Interestingly, NIHL had different effects on the gap detection in the two strains of mice as indicated by a significant strain-by-session interaction (ANOVA, $F_{2,14} = 13.98$, $p < 0.001$). Although the gap detection performance was similar across two strains before NIHL, strain differences emerged after NIHL, with C57BL/6 showing worse gap detection than FVB ($p < 0.01$ for 7, 10, 14 & 20 kHz at d2, $p < 0.01$ for 10, 14 & 20 kHz at d10, unpaired t-test). A comparison of each individual animal's behaviors pre- and post-NIHL confirmed that while NIHL significantly impaired gap detection in C57BL/6 (Fig 3.1b bottom & 1d: paired t-test, $p < 0.05$ for 7, 10, 14 & 20 kHz at d2 and $p < 0.05$ for 10 & 20 kHz at d10), it improved gap detection in FVB (Fig 3.1c bottom & 1d: paired t-test, $p < 0.05$ for 5 kHz &10 kHz at d2 and $p < 0.05$ for 14 kHz at d10).

To further confirm that impairment of gap detection indicates tinnitus, not hearing impairments, we tested pre-pulse inhibition (PPI) behavior in a separate group of C57BL/6 (n = 7) and FVB (n = 7) mice after the same NIHL procedure as the previous experiment (see Method for difference between gap detection and PPI task). NIHL did not affect PPI in either C57BL/6 or FVB (ANOVA, session, $F_{2,11} = 1.58$, $p = 0.25$, Fig 3S.3). In addition, no strain difference was observed in PPI (ANOVA, session-by-strain interaction, $F_{2,11} = 2.7$, $p = 0.11$).

Given this specific impairment of gap detection in C57BL/6, but not in FVB, we concluded that C57BL/6 are susceptible to hearing loss-induced tinnitus, whereas FVB are tinnitus-resistant.

Strain differences in cortical GAD65 expression after NIHL

Previous studies have implicated GAD65 regulation in tinnitus(Yang, Weiner et al. 2011). To determine if the strain difference in tinnitus susceptibility is related to differential modulation of GAD65 by NIHL, we quantified its expression in the auditory cortex of mice after the tinnitus test. Brain tissue samples were taken from the left and right (ipsilateral and contralateral to the noise-exposed ear) auditory cortices of C57BL/6 (n = 10) and FVB (n = 7). The level of GAD65 mRNA was measured by reverse transcription polymerase chain reaction (RT-PCR).

We observed a significant strain difference in how unilateral NIHL affected GAD65 expression (Fig 3.1e: ANOVA, cortical side, $F_{1,15} = 25.43$, $p < 0.001$; side-by-strain interaction $F_{1,15} = 9.34$, $p = 0.008$). A post-hoc unpaired t-test revealed that, compared to FVB, C57BL/6 had a lower GAD65 mRNA level in the (right) cortex contralateral to the noise-exposed ear ($t_{15} = 2.71$, $p = 0.02$). Such a difference was not present for the (left) cortex ipsilateral to the noise-exposed ear. Comparing within each strain, C57BL/6 showed lower GAD65 expression on the right side compared to the left side (paired t-test, $t_9 = 5.25$, $p = 0.001$), while FVB did not (paired t-test, $t_6 = 2.69$, $p = 0.07$).

Induction of tinnitus in the tinnitus-resistant strain by GAD65 knockdown

To test whether cortical GAD65 knockdown alone is sufficient to induce tinnitus, we performed a posttranscriptional knockdown of GAD65 expression using a small hairpin RNA (shRNA) (Fig 3.2a). GAD65 knockdown experiments were performed on normal hearing FVB that had never undergone NIHL. Tinnitus symptoms were identified using a gap detection task. A second GAD65 knockdown experiment, described below, validates the results using an additional mouse strain and an alternative behavioral task.

Lentivirus particles carrying GAD65 shRNA were injected in the right auditory cortex of the FVB (n = 10). Control FVB (n = 7) underwent identical surgical procedures and were injected with lentivirus particles carrying shRNA of non-gene-specific scrambled sequences. Gap detection behavior was examined in two sessions: pre-injection and 14 days post-injection. ABRs were examined 15-20 days after injection in a subset of the mice that underwent behavioral tests.

Virus injection and cortical GAD65 knockdown did not alter the ABR threshold (Fig 3.2b-c top), peak latency or peak amplitude (Fig 3S.4) in signals recorded from left or right ear after shRNA injection (GAD65 knockdown, n = 7; scrambled sequence, n = 5). The startle amplitude for uncued trials did not differ between pre- and post-injection sessions, or between the GAD65 knockdown and the scrambled control groups ($p > 0.19$ for all frequencies, paired and unpaired t-tests). Gap detection, as measured by the cued-over-uncued startle response ratio, was similar across groups before the injection (ANOVA, virus type-by-frequency interaction, $F_{4,13} = 0.29$, $p = 0.88$). However, it was significantly impaired by GAD65 knockdown but not by the injection of the scrambled sequences (Fig 3.2b-c bottom & 2d: ANOVA, session-by-virus type interaction $F_{1,16} = 4.64$, $p = 0.047$). Post-hoc paired t-test confirmed the impaired gap detection in the GAD65 knockdown group (Fig 3.2b bottom: $p < 0.05$ for 7 kHz and 20 kHz).

The specific and effective GAD65 knockdown was verified in a subset of the mice (FVB GAD65 shRNA, n = 8; FVB scrambled shRNA, n = 5) after the tinnitus test. Significantly greater reduction of GAD65 mRNA was confirmed in the injected side of the GAD65-knockdown group (Fig 3.2e: ANOVA, cortical side, $F_{1,11} = 41.58$, $p < 0.001$; cortical side-by-group interaction $F_{1,11} = 8.21$, $p = 0.02$). GAD65 level was unaltered in intact side in both groups. A post-hoc t-test of group difference (GAD65 shRNA vs. scrambled shRNA) confirmed lower GAD65 level in the injected right cortex in GAD65

shRNA group (unpaired t-test; $t_{11} = 3.15$, p = 0.009) and no group difference in the intact left cortex. Comparing within each group indicated that relative to the intact side, GAD65 expression was knocked down by GAD65 shRNA (paired t-test: $t_7 = 8.59$, $p < 0.001$) but not by scrambled shRNA.

Comparing between the GAD65-knockdown mice and NIHL mice, we found no significant difference in GAD65 mRNA levels in the NIHL affected (right) cortex of C57BL/6 and the GAD65 shRNA injected (right) cortex of FVB (unpaired t-test: $t_{16} = 0.87$, $p = 0.4$), indicating that NIHL and GAD65 shRNA injection procedures resulted in similar levels of GAD65 reduction in the affected auditory cortex. These results show that artificial GAD65 knockdown in the auditory cortex is sufficient to induce tinnitus in the tinnitus-resistant FVB with normal hearing.

Correlation between tinnitus and cortical GAD65 reduction

We observed both individual and strain differences in the behavioral measure of tinnitus and the downregulation of cortical GAD65 expression, in both virus-injected and noise-exposed mice. To test whether there was an overall correlation between tinnitus and cortical GAD65 regulation, we pooled together data from all the mice with both measures (C57BL/6 NIHL: n = 10, FVB NIHL: n = 4, FVB GAD65 shRNA: n = 8, FVB scrambled shRNA: n = 5). We found a significant linear correlation between the mean behavior change and GAD65 mRNA reduction in the affected (right) cortex (Fig 3.3, one-tailed Pearson correlation, $r = -0.47$, $n = 27$, $p = 0.013$). A similar correlation was found for the active avoidance task (Fig 3.4d, and next section).

Behavioral evidence of tinnitus measured with an active avoidance task

Although the gap detection method has been widely used to quantify tinnitus, there are lingering questions as to whether performance on it is influenced by processes unrelated to tinnitus (see Discussion). To validate our behavioral results, we measured putative tinnitus using a conditioning-based procedure adapted from a previous report(Yang, Weiner et al. 2011). Tg(dlx6a-cre)1Mekk mice were used for this experiment. Like C57BL/6, this mouse strain showed GAD65 mRNA and protein downregulation in the auditory cortex after NIHL (Fig 3S.5).

Mice were trained to cross between the two compartments of a shuttle box when a tone was played (Fig 3.4a). Crossing behavior during silent probe trials was assumed to be tinnitus-triggered false alarms (Fig 3.4b). The average number of crosses during silent probe trials was normalized to the average number of crosses during sound probe trials to account for individual differences in motivation and motor activity (see *Methods* for details). Training was performed until animals reach a criterion of 70 % accuracy, which took up to two weeks. Performance was maintained throughout the duration of all test sessions (Fig 3S.6a).

An increase in tinnitus-triggered false alarms was observed after NIHL, supporting the interpretation of impaired gap detection as a symptom of tinnitus. After NIHL, mice

showed more crossing during silent periods (one-tailed paired t-test, $t_4 = -3.53$, $p = 0.01$, Fig 3S.6b) and a significant increase in tinnitus score (i.e. ratio of silent-over-sound crossing) (Fig 3.4c NIHL, one-tailed paired t-test, $t_4 = -2.95$, $p = 0.02$).

GAD65 knockdown-mediated tinnitus confirmed by the active avoidance task

To validate GAD65 knockdown-mediated tinnitus with the active avoidance task, we conducted GAD65 knockdown in the right auditory cortex in ten Tg(dlx6a-cre)1Mekk with normal hearing and compared tinnitus behavior before and 15-20 days after the virus injection. We aimed for a GAD65 knockdown roughly equivalent to the level that was observed in noise-exposed mice (approx. 40%). Therefore, we only included mice with greater than 40% GAD65 knockdown (n = 6) in this analysis. Mice with GAD65 knockdown showed a similar tendency of increased crossing during the silent periods (one-tailed paired t-test, $t_5 = -4.01$, $p < 0.01$, Fig 3S.6c) and increased tinnitus score (Fig 3.4c GAD65 knockdown, one-tailed paired *t*-test, $t_5 = -4.87$ $p = 0.002$), suggesting they were perceiving tinnitus.

We also analyzed if the amount of GAD65 downregulation correlates with the severity of tinnitus by including all animals that underwent GAD65 shRNA injection and behavioral testing (n = 10). We found that GAD65 knockdown was highly correlated with tinnitus quantified using our active avoidance task (one-tailed Pearson correlation, $r = 0.88$, $n = 10$, $p < 0.001$, Fig 3.4d). These results are consistent with results obtained with the gap detection, and strengthen our conclusion that downregulation of GAD65 in the auditory cortex is correlated with tinnitus in animal models.

Tinnitus is not associated with distortion in the AI frequency map

Our findings raise the question of how GAD65 downregulation affects the primary auditory cortex (AI) sensory map and the response properties of AI neurons. To address this, we conducted bilateral AI recordings in noise-exposed and virus-injected FVB and C57BL/6 mice using pure tones spanning 4 to 64 kHz.

NIHL expanded the A1 frequency representation near the 8 kHz noise exposure frequency. Frequency representation was characterized by the proportion of multiunit tuned to a low (8-16kHz) and high (16-32 kHz) octave range. In C57BL/6 and FVB with NIHL, NIHL-affected (right) AI of both strains showed increased low frequency (8-16 kHz) representation relative to the (left) AI ipsilateral to noise exposed ear (ANOVA, $CF_{8\text{-}16\ kHz}$ percentage, $F_{1,7} = 4.9$, $p = 0.03$, Fig 3.5a-b and Fig 3S.7). Equivalent effects were observed in both strains (ANOVA CF $CF_{8\text{-}16kHz}$ percentage-by-strain interaction, $F_{1,7} = 0.092$, $p = 0.77$).

Multiunit response thresholds were higher for the NIHL-affected (right) AI compared to the left AI after controlling for the CF distribution differences (Fig 3.5c: analysis of covariance (ANCOVA) threshold, $F_{1,5} = 22.53$, $p = 0.005$, post-hoc paired t-test, FVB: $p = 3.09 \times 10^{-4}$, C57BL/6: $p = 1.49 \times 10^{-5}$). The amount of threshold shift was comparable between the two strains (ANCOVA, threshold-by-strain interaction, $F_{1,5} = 1.45$, $p = 0.28$).

While these changes are present in both strains, only C57BL/6 developed tinnitus. Taken together, our results suggest that NIHL, but not tinnitus, is associated with an expansion of AI low frequency representation and an increase in the response threshold of AI multiunits.

In contrast to the altered frequency map organization following NIHL, AI map change was absent in FVB regardless of the virus type (GAD65 shRNA or scrambled shRNA). Orderly tonotopy spanning 8-32kHz was maintained in both groups. Proportion of low (8-16 kHz) and high (16-32 kHz) frequency representations was similar between injected (right) cortex and uninjected (left) cortex (ANOVA, $CF_{8\text{-}16\ kHz}$ percentage, $F_{1,9} = 3.10$, $p = 0.11$; Fig 3.6a and Fig 3S.8). Despite the absence of the map change, FVB with cortical GAD65 knockdown developed tinnitus. This dissociation further confirms that sensory map reorganizations are not necessary for tinnitus development. Cortical response thresholds were also comparable between the injected and intact AI (ANOVA, threshold, $F_{1,9} = 0.70$, $p = 0.43$, Fig 3.6b).

GAD65 knockdown reduces the AI receptive field size

Acute pharmacological blockage of gamma-aminobutyric acid (GABA) synapses has been shown to increase responsivity in both spectral and intensity dimensions (Wang, McFadden et al. 2002). However, cortex-specific chronic reduction of inhibition has been shown to reduce the receptive field size (Seybold, Stanco et al. 2012). In order to examine the spectral-intensity responsiveness following a localized downregulation by shRNA, we quantified the median frequency response area (FRA) size. The cortex with shRNA-mediated GAD65 reduction showed smaller threshold-adjusted FRAs than the uninjected cortex ($t_5 = 3.21$, $p = 0.02$ paired t-test, Fig 3.6c). Similar reductions of FRA have been reported in mice with chronic reduction of cortical inhibition(Seybold, Stanco et al. 2012).

Sound-evoked and spontaneous firing rates

Evoked firing was defined as the multiunits' mean firing in the duration where the PSTH is above half of the maximum. In noise-exposed C57BL/6 and FVB, the NIHL-affected (right) AI showed significantly lower evoked FR compared to the left AI (ANOVA, evoked FR: $F_{1,7} = 36.40$, $p = 0.001$, post-hoc paired t-test, C57BL/6: $t_4 = 4.01$, $p = 0.02$, FVB: $t_3 = 8.29$, $p < 0.01$ Fig 3.7a). The reduction of evoked FR was equivalent between strains (ANOVA, evoked FR-by-strain interaction: $F_{1,7} = 0.83$, $p = 0.39$). In GAD65 knockdown and scrambled-sequence control mice, no statistically significant difference in evoked firing rates was found between the injected and intact sides (ANOVA, evoked FR: $F_{1,9} = 0.76$, $p = 0.4$, Fig 3.7a).

Spontaneous firing was recorded in a silent five minute block following the sound stimulation block, while maintaining the same electrode locations and the spike threshold. AI multiunits with CFs between 8-32 kHz were included in the calculation of spontaneous rate. A reduction in spontaneous firing rate was observed in the cortical side with GAD65 downregulation, compared to the intact side—both in the NIHL case and

artificial GAD65 knockdown case (C57BL/6: $t_4 = 2.94$, $p = 0.04$, FVB GAD65: $t_5 = 3.40$, $p = 0.02$, paired t-test, Fig 3.7b). A similar reduction in spontaneous FR was confirmed in the sound presentation blocks when FR was evaluated in the 50 ms silent period immediately preceding the stimulus presentation (C57BL/6: $t_4 = 2.61$, $p = 0.03$, FVB GAD65: $t_5 = 2.76$, $p = 0.02$, one-tailed paired t-test). Thus, reduction in spontaneous firing was observed both in prolonged (5 min) and short (< 333 ms) silent periods.

Discussion

Hearing loss alters neuronal inhibition along the central auditory pathway (Abbott, Hughes et al. 1999, Kotak, Fujisawa et al. 2005, Dong, Mulders et al. 2009, Dong, Rodger et al. 2010, Middleton, Kiritani et al. 2011, Wang, Brozoski et al. 2011, Yang, Weiner et al. 2011, Llano, Turner et al. 2012, Takesian, Kotak et al. 2013). For example, GAD expression levels and inhibitory synaptic transmission are reduced in the cochlear nucleus, inferior colliculus, and auditory cortex in animals with hearing loss-induced tinnitus (Abbott, Hughes et al. 1999, Milbrandt, Holder et al. 2000, Kotak, Fujisawa et al. 2005, Dong, Mulders et al. 2009, Roberts, Eggermont et al. 2010, Kaltenbach 2011, Middleton, Kiritani et al. 2011, Wang, Brozoski et al. 2011, Yang, Weiner et al. 2011, Browne, Morley et al. 2012, Llano, Turner et al. 2012). While neuronal inhibition is reduced in many auditory brain regions in animals with hearing loss-induced tinnitus, the co-occurrence does not necessarily indicate a causal relationship between the two (Brozoski and Bauer 2005). In our study, we found that 1) cortical downregulation of GAD65 expression was correlated with the severity of tinnitus as measured by two behavioral tasks; and 2) localized knockdown of cortical GAD65, to a level that was observed in noise-exposed mice, caused tinnitus in normal hearing animals. These results suggest a critical role of cortical GAD65 downregulation in noise-induced tinnitus(Yang, Weiner et al. 2011, Llano, Turner et al. 2012).

Sensory map reorganization has been considered as a potential mechanism underlying tinnitus, since abnormal auditory cortex activation and cortical map reorganization are correlated with the occurrence and severity of tinnitus in human patients and in animal models (Muhlnickel, Elbert et al. 1998, Norena and Eggermont 2005). In addition, hearing loss associated with tinnitus leads to altered spontaneous activity and map reorganization, both of which can be prevented if the trauma is followed by enriched acoustic experience (Komiya and Eggermont 2000, Seki and Eggermont 2003, Norena and Eggermont 2005, Engineer, Riley et al. 2011). In our study, both strains of mice that underwent noise-exposure showed an expansion of low (8-16 kHz) frequency representation but only one strain developed tinnitus. Further, GAD65 knockdown mice that also had tinnitus did not show sensory map changes. Therefore, sensory map change is likely causally related to the hearing loss, but not to tinnitus. Our results are consistent with recent findings that macroscopic sensory map changes are not necessary for tinnitus(Langers, de Kleine et al. 2012).

The GAD65 protein accounts for approximately 50% of the total amount of GAD expressed in the cerebral cortex (Sheikh, Martin et al. 1999). GAD65 expression is preferentially localized in axonal terminals, is modulated by activity and sensory input,

and influences the amount of GABA release and the level of neuronal activity (Esclapez, Tillakaratne et al. 1994, Patel, de Graaf et al. 2006). Complete knockout of the GAD65 gene leads to epileptic activity in the neocortex, indicative of a general increase in neuronal excitability (Kash, Johnson et al. 1997). Here we show that a 40% GAD65 reduction by virus-mediated gene knockdown in auditory cortex is sufficient to cause tinnitus.

A potential consequence of such a drastic reduction of GAD65 expression in the cortex is reduced GABA release and associated reductions in phasic and tonic inhibition (Yang, Weiner et al. 2011). Reduced tonic inhibition may lead to higher input resistance and increased neuronal excitability (Yang, Su et al. 2012). However, in this study, animals with GAD65 knockdown showed lower spontaneous activity and smaller receptive field size in the auditory cortex 20-30 days after the manipulation. Although unexpected, it is possible that GAD65 downregulation is followed by secondary postsynaptic compensatory changes, such as sensitization of GABA receptors through modification of subunit compositions and functions as previously reported (Caspary, Holder et al. 1999). In addition, our findings are consistent with those of a recent report showing reduced FRA after chronic reduction in cortical inhibition in conditional *Dlx* knockout mice (Seybold, Stanco et al.). Taken together, these results suggest that acute and chronic reduction in inhibition may differentially impact cortical excitability and responses. Cellular mechanisms underlining our spontaneous firing rate results remain to be determined.

In our study, while reduced sound-evoked responses were correlated with hearing loss, reduced spontaneous activity appeared to be correlated with tinnitus. The results were surprising given that tinnitus had previously been associated with increased spontaneous activity (Komiya and Eggermont 2000, Seki and Eggermont 2003, Schaette and Kempter 2006, Roberts, Eggermont et al. 2010, Kaltenbach 2011). The fact that reduced spontaneous activity occurred in both noise-exposed C57BL/6 and GAD65-knockdown FVB suggests that the result was not due to a specific type of manipulation. We should be cautious interpreting these results because the recordings were acquired under anesthesia and many not directly relate to tinnitus behavior. However, several previous studies have also reported reduced spontaneous cortical activity and local field potential power in awake animals after tinnitus induction (Yang, Lobarinas et al. 2007, Norena, Moffat et al. 2010).

Human genetic studies have indicated low heritability of tinnitus (Kvestad, Czajkowski et al. 2010), which is consistent with a major role played by environmental factors—such as noise trauma and ototoxic drug use—in tinnitus etiology (Henry, Dennis et al. 2005). However, since the causes of tinnitus are heterogeneous, the low overall heritability does not exclude the possibility of higher heritability of some subtypes of tinnitus. Furthermore, low heritability of tinnitus does not exclude the possibility of higher heritability of resistance to hearing loss-related tinnitus, as we have seen in the FVB. Tinnitus is linked to several genes (Sand, Langguth et al. 2007, Sand, Langguth et al. 2012, Sand, Langguth et al. 2012), some of which, such as the auxiliary GABA-B receptor subunit gene potassium channel tetramerization domain containing 12

(KCTD12) and the brain-derived neurotrophic factor (BDNF) gene, are linked to the function of inhibitory neurons (Huang, Kirkwood et al. 1999, Sand, Langguth et al. 2012, Sand, Langguth et al. 2012). It remains to be determined whether the GAD65 gene and its regulation mechanisms are linked to tinnitus or its resistance in humans.

Modified cortical GAD65 expression patterns have been observed in human patients with schizophrenia—a disorder associated with auditory processing deficits (Dracheva, Elhakem et al. 2004). Notably, a recent study reported a reduction of GAD65 protein in the inhibitory boutons in the primary auditory cortex of schizophrenia patients (Moyer, Delevich et al. 2012). This finding is interesting given our results linking cortical GAD65 downregulation with an auditory phantom perception. Potential involvement of GAD65 in these two disorders and its implication to auditory perception remains to be determined.

In contrast to the large strain differences in hearing loss-induced tinnitus, within-strain variability in our study is small. All the eight C57BL/6 with NIHL showed an impaired gap detection and a sign of tinnitus. Previous studies reported higher inter-subject variability. For example, not all animals with NIHL exhibit behavioral signs of tinnitus (Middleton, Kiritani et al. 2011). Although the precise causes of this discrepancy are unknown, potential source of variability may be the degree of hearing impairment introduced to the animals. To avoid the confounding factor of hearing loss in the measurement of tinnitus, researchers often choose mild, transient or spectrally narrow-range hearing loss in model animals. Animals in those studies may be close to a threshold of tinnitus development, resulting in only a fraction showing measurable signs of tinnitus. This notion is supported by findings that tinnitus behaviors are correlated with the degree of persistent hearing loss in animal models (Tan, Ruttiger et al. 2007). The hearing lesion procedures of prolonged noise exposure in our study may have resulted in more consistent hearing impairment and hence the induction of tinnitus.

Gap detection has been proposed as a simple behavioral test for tinnitus in rodents (Turner, Brozoski et al. 2006) and consistent patterns of gap detection impairment have been shown in human tinnitus patients (Fournier and Hebert 2013). As this behavioral test is gaining popularity(Pace and Zhang 2013), some questions remain to be addressed. One of the major concerns is whether the gap detection behavior is altered by hearing loss, rather than, or in addition to, tinnitus(Lobarinas, Hayes et al. 2013). In our study, we observed no impairment in gap detection in the FVB that had substantial unilateral hearing loss. In contrast, the FVB that had cortical GAD65 knockdown were impaired in gap detection without changes in the ABR thresholds, peak latency, and peak magnitude. The double-dissociation between hearing loss and impaired gap detection indicate that unilateral hearing loss does not necessarily impair gap detection. A second question about gap detection is whether it is modulated by thalamocortical circuits (Kaltenbach 2011, Eggermont 2012). Previous cortical deactivation studies have suggested cortical involvement in resolving short duration (<75 ms) silent gap detection in rodents(Syka, Rybalko et al. 2002, Threlkeld, Penley et al. 2008). In our study, FVB with cortical knockdown of GAD65 are significantly impaired in gap detection. The shRNA-mediated GAD65 knockdown in the auditory cortex appeared to be localized in the cortex, and does not alter GAD65 expression in the inferior colliculus through corticofugal

projections (Fig 3S.9). These results suggest that gap detection is modulated by the auditory cortex. A third concern with the gap detection is the reduction of acoustic startle responses after NIHL(Lobarinas, Hayes et al. 2013). We have observed similar reduction of startle responses after NIHL. However, the startle response amplitude did not correlate with the tinnitus score, thus the reduction in startle amplitude was unlikely to have confounded our tinnitus measurements.

Several recent studies have examined hearing loss-induced tinnitus in different strains of mice(Longenecker and Galazyuk 2011, Middleton, Kiritani et al. 2011, Llano, Turner et al. 2012). While genetically manipulated mice can be useful in dissecting neural mechanisms of tinnitus, the interpretation of the results should take into consideration the genetic background of the mice. The lack of hearing loss-induced GAD65 downregulation in FVB indicates that they may be impaired in this particular form of homeostatic plasticity. Some other inbred strains have also been shown to be impaired in homeostatic synaptic plasticity in the neocortex(Ranson, Cheetham et al. 2012). C57BL/6 have been shown to have higher susceptibility to neuropathic pain(Mogil, Lichtensteiger et al. 1998) and are used widely in pain research. Involvement of GAD65 in the etiology of neuropathic pain(Zhang, Cai et al. 2011) provides a possible link to our findings.

Despite intense research efforts, the neural substrates and mechanisms underlying hearing loss-induced tinnitus have so far been elusive. A major obstacle has been the difficulty in dissociating the mechanisms underlying tinnitus from consequences of hearing loss. Taking advantage of the strain differences between C57BL/6 and FVB, we provide evidences that the auditory cortex is a neural substrate for hearing loss-induced tinnitus, and that homeostatic reduction of cortical GAD65 expression plays a pivotal role in tinnitus etiology(Norena and Eggermont 2005, Eggermont 2008, Engineer, Riley et al. 2011, Yang, Weiner et al. 2011, Llano, Turner et al. 2012, Yang and Bao 2013). In addition, sensory map reorganization is likely a consequence of altered sensory inputs rather than a cause of the phantom sensation, as has been widely hypothesized(Flor, Elbert et al. 1995, Engineer, Riley et al. 2011). These findings suggest that new strategies should be sought for rehabilitation of phantom sensation.

Methods

All experimental procedures were reviewed and approved by the UC Berkeley Animal Care and Use Committee. Three strains of mice—FVB.129P2-Pde6b+ Tyrc-ch/AntJ, C57BL/6J, and Tg(dlx6a-cre)1Mekk (the Jackson Laboratory), between P60 and P100 were used in all experiments. For NIHL, C57BL/6 (n = 20, male, P72 ± 5 on the day of NIHL) and FVB (n = 20, male, P70 ± 5 on the day of NIHL) were used. Due to an equipment calibration issue, gap detection data from three FVB and five C57BL/6 were excluded, but their GAD65 data were included in the analysis. For the GAD65 knockdown experiment, two groups of FVB were used (exp: n = 10, P81 ± 14 on the day of injection, ctrl: n = 8, P67 ± 8 on the day of injection). Auditory brain stem response (ABR) recordings and electrophysiological mappings were conducted on a subgroup of animals, and the number for each experiment is reported in the result section. For conditioned active avoidance behavior experiments, total of 23 Tg(dlx6a-cre)1Mekk of

either sex were used, and the number for each experiment is reported in the result section.

Noise-induced hearing loss (NIHL) and auditory brainstem response (ABR)

Animals were anesthetized with ketamine (100 mg/kg, IP) and xylazine (10 mg/kg, IP), and maintained at 36.5°C with a homeothermic heating pad (Harvard Apparatus). Unilateral NIHL was induced by playing a continuous 8kHz pure tone at 112 dB SPL through a custom-made piezoelectric earphone speaker to the left ear for 2 hours. The right ear was protected with sound attenuating clay. The sound level was measured with a Bruel and Kjaer 4135 condenser microphone (Nærum, Denmark).

Hearing thresholds were assessed under anesthesia using ABR immediately before and after (5, 15 and 20 days) the noise exposure procedure. ABR signals were recorded using the BioSigRP software on a TDT RX5 Sys3 recording rig. Tone pips (3 ms full-cycle sine waves at 4, 8, 16 and 32 kHz at 5 dB intensity steps from 0 to 70 dB) were delivered to a single ear through a cannulated speaker at a rate of 19 times per second. The speaker was calibrated to have < 3% harmonic distortion and flat output in the entire frequency range (Tucker-Davis Technologies SigCal32). 500 recordings were averaged for each frequency intensity pair.

ABR signals were recorded with electrodes subcutaneously inserted at three locations: behind the ear coupled with the speaker, at the vertex of the head, and near the base of the tail. ABR waveforms at each sound level were visually inspected online by the experimenter. ABR threshold was defined as the sound level at which one or more peaks were distinguishable by eye against the background activity. The amplitude and magnitude of ABR peak I to V at 60 dB SPL were reanalyzed offline. For offline analysis, peaks and troughs of the ABR trace were automatically identified by a custom MATLAB script. Peak latencies were defined using the time points at which peaks I to V occurred. Peak magnitude was defined as the voltage difference between a peak and preceding trough. ABR threshold, latency and magnitude at each tested frequency were compared using analysis of variance (ANOVA) and followed by post-hoc t-tests.

Behavioral test of tinnitus with a gap detection task

During the testing session, a mouse was caged in a plastic container with a mesh lid. The container was placed on a piezoelectric disc in a sound attenuation chamber. Sounds were played through an open field speaker (FOSTEX FT17H) fixed above the cage. The gap detection measures the acoustic startle response elicited by a brief white noise pulse and its suppression by a preceding silent gap embedded in the background sound. Each trial starts with a carrier pure tone (frequency pseudorandomly selected from 5, 7, 10, 14, 20, 28, or 45 kHz, all at 75 dB SPL), played for a duration of 10-20 s. In uncued trials, the carrier tone was followed by a startle stimulus—a 50 ms white noise burst at 102 dB SPL. In cued trials, the startle stimulus was preceded by a 50 ms silence, 100 ms prior to the onset. In each testing session, the animal performed a total of 500 trials (50% cued and 50% uncued). After each session, we calculated the startle response ratio, which is defined as the average startle amplitude to the silent gap-cued trials divided by the

average amplitude of the uncued trials. The startle response ratio signifies a silent-gap induced reduction of the startle response. For example, a startle response ratio of 0.6 indicates a 40% reduction of the startle amplitude for the cued trials. A startle response ratio of 1 suggests that the animal failed to detect the silent gap.

To access an animal's ability to perform an auditory task, separate from its ability to detect a silent gap, the pre-pulse inhibition (PPI) task was administered in a separate group of mice immediately before and after (2 d and 10 d) NIHL. The physical setup for the PPI task was identical to that of the gap detection. However, the trial structure differed in that carrier tone was absent and a white noise burst was cued by a 50 ms pure tone pulse (frequency pseudorandomly selected from 5, 7, 10, 14, 20, 28, or 45 kHz, all at 75 dB SPL). In short, the PPI task tests an animal's ability to detect a pure tone pulse in silence, while the gap detection task measures an animal's ability to detect a silent gap in a continuous pure tone.

Mice were first acclimated to the testing chamber and trained until the behavior stabilized across two days. On average, 1000 trials were given prior to the first test session. We compared individual animals' performance before and after the experimental manipulation. An increase of gap ratio accompanied by i) normal ABR for the intact ear and ii) normal PPI behavior were assumed to indicate tinnitus. Because both the gap detection task and the PPI task require normal hearing and hearing sensitivity was highly variable across animals above 32 kHz, only trials with carrier frequencies between 5 and 20 kHz were included in the final analysis.

Lentivirus injection in auditory cortex

Posttranscriptional gene silencers were used to manipulate the level of GAD65 expression. A lentivirus carrying an shRNA (Santa Cruz Biotechnology, Inc.) sequence complementary to mouse GAD65 mRNA was used to knock down GAD65 expression. To account for possible tissue damage from cortical microinjection or viral infection, a lentivirus carrying a non-gene-specific scrambled shRNA sequence (Santa Cruz Biotechnology, Inc.) was used as a control. Mice were anaesthetized with ketamine (100 mg/kg IP) and xylazine (10 mg/kg IP). Injection was done stereotactically to the right auditory cortex. A burr hole was made on the temporal ridge 1.75 mm anterior from the junction between the temporal ridge and the transverse suture. A micropipette filled with the virus solution was lowered down 500 μm from the pial surface and 1 μl of virus solution was injected at 100 nl/min by pressure injection (Stoelting Quintessential Injector, Wood Dale, IL, USA). The micropipette was then retracted 250 μm and an additional 1 μl of virus solution was injected. To minimize leaking, the micropipette was left in place for 8 min before being withdrawn. After injection, the skin was sutured and the animals were returned to their home cages after regaining movement. For postoperative pain management, animals received subcutaneous injection of buprenorphine (0.05 mg/kg, SQ) and meloxicam (2 mg/kg, SQ).

Conditioned active avoidance behavioral measure of tinnitus

In addition to gap detection and PPI, we trained a separate set of animals on a third conditioning-based task—a modified version of an active avoidance task(Yang, Weiner et al. 2011). PPI and gap detection depends on a presence of an animal's startle response, which can be affected by a hearing loss (see Lobarinas, Hayes et al. 2013 and Results). The active avoidance task was used to validate our gap detection results since it uses animal's voluntary movement (i.e. shuttle box chamber crossings) during silent probe trials as an index of presumed tinnitus, and does not rely on acoustic startle response.

Training took place in a two-compartment shuttle box separated by a barrier with a narrow open door connecting the two compartments. The shuttle box was equipped with a grid floor connected to a scrambled shock generator (MED Associates, Inc.), and was located in a sound attenuation box. Animals were first habituated in the shuttle box for two 1 hour daily sessions, followed by 1-2 weeks of training in the active avoidance task.

Each daily training session consisted of 60 trials. A total of nine sounds were used in the active avoidance training and tinnitus testing: five pure tones (4, 8, 16, 20, 32 kHz) and four octave-band noise (4-8, 8-16, 10-20, 16-32, kHz) played at four intensities (30, 40, 50, 60 dB). Due to the small trial numbers in each condition, accuracy was calculated across all frequency-intensity pairs. Each trial started with a holding period of 5 to 40 seconds, during which the animal had to stay in one side of a two-compartment shuttle box. At the end of the holding period, a sound was played, and the animal had to respond within 7 seconds after the sound onset by moving through the small open door into the other side of the shuttle box. If the animal successfully crossed the door within 7 seconds of sound onset, the sound was stopped and a new trial was automatically initiated. If the animal failed to cross through the door within the allowed time window, a mild foot shock (0.4 mA for 1 s) was delivered once every 5 seconds until the cross was made. The sound was terminated as soon as the animal crossed into the other side of the shuttle box and a new trial was automatically started. To facilitate the learning process, false positive crosses during the holding period were not punished during the first few training sessions. False positive trials were aborted, and a new trial was automatically initiated. After the animal reached a performance level of 50% avoidance, it received a single foot shock for each false positive cross. The trial was then aborted, and a new trial was automatically initiated. False positive trials were not counted. It took 1-2 weeks for an animal to reach a criterion of 70% avoidance in three consecutive sessions.

After animals reached the 70% criterion, they underwent six daily testing sessions. In each testing session, unreinforced probe trials (10 silent and 2 sound probe trials, both 1 minute long) were introduced and randomly mixed with 48 reinforced trials. Because animals tended to cross fewer times in silent probe trials, we included more silent than sound probe trials (10 to 2) to obtain more accurate measurements. Frequency and intensity of the sound probe trial was randomly chosen from those used in the training. To avoid extinction of learned responses, we only included a small number (12) of these unreinforced probe trials in each test session. A sound was played during the entire 1 min duration of the sound probe trial, whereas no sound was played during the entire 1 min duration of the silent probe trial. Animals were allowed to either stay in one compartment or cross into the other side freely during these probe trials. Due to a lack of feedback,

such as the foot shock upon incorrect crossing or the termination of sound upon correct crossing, mice tended to make multiple crosses during the 1 min probe trials. The total number of crosses in each trial, and not the binary presence or absence of the crosses per trial, was recorded. Six test sessions were conducted per animal, yielding 60 silent and 12 sound probe trials.

The number of crosses in silent probe trials measures the likelihood that the animal was hearing tinnitus, but might also be influenced by the animal's motivation and motor activity, which were assessed with the number of crosses in the sound probe trials. To control for these factors, the average per-trial-crosses of the silent probe trials were divided by the average per-trial-crosses of the sound probe trials at the end of each testing session. The baseline behavioral score was calculated by taking an average of this silent-over-sound cross ratio across six sessions.

Once the baseline behaviors were recorded, animals received either unilateral NIHL or a cortical microinjection of GAD65 shRNA. Fifteen days later, animals received another 6 days of tinnitus testing, using the same procedure as described before. An increase of the silent-over-sound cross ratio after NIHL or GAD65 knockdown was considered evidence of tinnitus perception.

Measuring GAD65 mRNA levels with RT-PCR

After behavioral testing, animals were euthanized with isoflurane. Brain tissue was collected from the right and left auditory cortices based on anatomical landmarks by an experienced experimenter (S.Y.). A coronal slice of approximately 1mm thickness (estimated stereotaxic coordinates: -2 mm to -3 mm bregma) was made using the dorsal-ventral extent of the hippocampus as landmarks. We then hemisected and isolated the auditory cortex at each side by making two orthogonal cuts to the cortical surface at 1 mm and 2 mm dorsal to the lingual gyrus. Subcortical structures were removed and two 1 mm cubes of cortical tissue, one from each side, were collected. These samples presumably included the primary auditory cortex and possibly other fields of the auditory cortex.

Reverse transcription polymerase chain reaction (RT-PCR) was conducted by an experimenter (SJ.C.) who was blind to the experimental conditions. Total RNA samples were prepared from the tissue with RNA Wiz (Ambion) according to the manufacturer's instructions. The total RNA obtained (~3μg) was reverse-transcribed using a first-strand cDNA synthesis kit (BD Biosciences, Palo Alto, CA). The PCR mixture (50 μl) contained 10× Taq buffer, 0.3 U Taq polymerase (Perkin-Elmer), 2.5 μM of dNTPs, 5 pmol of each set of primers, and 50 ng of cDNA from the auditory cortex as template. GAD65-specific fragments were amplified with the following PCR primers: GAD65-F: 5'-GCGCAGTTCTTGCTGGAAGTGGTAGACATA-3', GAD65-R: 5'-AGGGTTCCAGGTGACTGAATTGGCCCTTTC-3'. PCR reactions were performed under the following cycling conditions: an initial denaturation at 94° C for 5 min followed by 25-40 cycles of denaturation at 94°C for 30 s, annealing at 63°C for 30 s, and elongation at 72°C for 1 min with a final elongation step at 72°C for 10 min. A 10-μl

sample of each PCR reaction was removed after 25 cycles, while the remaining mixture underwent 5 more cycles of amplification. The extent of amplification was chosen empirically to avoid saturation of the amplified bands. In addition, two samples were collected for optimal quantification of GAD65 expression levels. Each primer set yielded a PCR product of 870 bp in length for GAD65. The 18S rRNA gene was used as an internal standard (QuantumRNA, Ambion). To quantify PCR products, each sample was run in a 1.5% agarose gel and stained with ethidium bromide. Band intensity was measured with an Alphaimager (Alpha Innotech Corp.) using the Alphaease (v3.3b) program.

Measuring GAD65 mRNA protein level with Western Blotting

The isolated auditory cortex tissues were prepared by homogenization in lysis buffer containing 50mMTris-HCl (pH 7.4), 150 mM NaCl, 1% Nonidet P-40 and protease inhibitor mixture (Roche). After gentle rotation for 3 h at 4°C, homogenates were centrifuged at 14,000 g for 60 min at 4°C and the supernatants were collected. Protein lysate (100 μg) was dissolved in SDS sample buffer containing 5% β-mercaptoethanol and heated to 95°C for 5 min. Equal amount of proteins were loaded on 10% SDS/PAGE and transferred onto nitrocellulose membranes. Membranes were blocked in Western Blocking Reagent (Roche) in PTN for 1 h at 4°C and incubated with 1:500 dilution of the anti-GAD65 or anti-α-tubulin primary antibody in PTN overnight at 4°C. Afterward, the blots were washed with PTN and incubated with horseradish peroxidase (HRP)-conjugated goat anti-rabbit or anti-mouse (1:5,000) (Jackson ImmunoResearch) in PTN for 2 h at 4°C. Immunoreactive bands were observed by using an enhanced chemiluminescence system. GAD65 band intensities were normalized to the band intensities of α-tubulin, which was used as a loading control.

Bilateral AI mapping and recording of spontaneous & evoked multiunit activity

The primary auditory cortex (AI) of each animal was mapped bilaterally 20-30 days after noise exposure or virus injection (C57BL/6 NIHL (n = 5), 20 ± 2 days post-procedure; FVB NIHL(n = 4), 26 ± 4 d; FVB GAD65 shRNA (n = 6), 23 ± 3 d; FVB scrambled shRNA (n = 5), 28 ± 1 d).

Animals were anesthetized with ketamine (100 mg/kg, IP) and xylazine (10 mg/kg, IP), and maintained at 36.5°C with a homeothermic heating pad (Harvard Apparatus). The anesthetized mouse was placed in a custom head holder and a slit was made in the cisterna magna to drain cerebrospinal fluid and reduce brain pulsations. A craniotomy and durectomy was performed over AI. A layer of silicon oil was applied to prevent brain desiccation. Sound stimuli were generated by an audio signal processor (Tucker-Davis Technologies RX6) and delivered to the ear contralateral to the craniotomy, through an enclosed cannulated speaker (Tucker-Davis Technologies Electrostatic Speaker, Coupler model). The speaker was calibrated to have < 3% harmonic distortion and flat output in the entire frequency range (Tucker-Davis Technologies SigCal32).

Multiunit responses of AI neurons were recorded using tungsten microelectrodes (FHC)

advanced orthogonally to the cortical surface to approximately cortical layer IV (350-400 μm). Electrical signals were amplified and recorded for each 333 ms trial (Tucker-Davis Technologies RX5). Prior to each recording block, search stimuli (white noise bursts, 60dB SPL, 25 ms duration, repeated at 3 Hz) were played to identify sound-evoked multiunit responses. Multiunit responses were defined as voltage changes that exceeded the mean amplitude of the baseline electrical trace by two standard deviations. Thresholds for multiunit discrimination were set for each microelectrode before each recording block. For each recording block of six minutes, pure tone pips of 51 frequencies were presented in pseudorandom order (4-64 kHz, 0.1 octave spacing, 5 ms cosine-squared ramps, 25 ms duration, repeated three times) at 8 intensities (0-70 dB SPL, 10 dB spacing), starting at 150 ms into the trial. Multiunit responses were used to reconstruct the frequency-intensity receptive field of each recording site and to calculate the tone evoked firing rate. To avoid a frequency sampling edge at 4 kHz and 64 kHz, only units with characteristic frequencies (CFs) between 8-32kHz were included in the analyses.

Following the sound presentation block, multiunit spontaneous activity was recorded while maintaining identical electrode location and threshold. We measured the spontaneous rate in a separate 5 min silent block, rather than the inter-stimulus periods in the sound presentation block, to minimize the influence of recent (< 333 ms) sound presentation on multiunit activity. The tone evoked firing rate was defined as the mean firing within the full duration at half maximum of each unit's peri-stimulus time histogram (PSTH) after subtracting the spontaneous firing rate. Spontaneous firing rate was defined as the mean firing for the entire duration (5 min) of the silent trials.

AI location was identified based on anatomical landmarks and response properties of the multiunit responses. Electrode penetrations were made densely and evenly throughout AI while avoiding surface blood vessels. Recording sites were marked on a magnified digital photograph of the cortex for later tonotopic map reconstruction.

After recordings were made on one side of the cortex, the craniotomy was covered with additional silicone grease and was sealed with a plastic film, and the mapping procedures were repeated on the other side. Surgery order for the two cortical sides was pseudorandomized across animals. All animals included in the cortical mapping experiment underwent bilateral AI mapping, and were euthanized at the end of mapping.

Characterization of receptive field properties

Frequency-intensity receptive fields (RFs) of each multiunit were constructed from the peak firing period of the PSTH. The peak firing period was defined as the full duration at half maximum of the PSTH after subtracting the spontaneous firing rate. The frequency response area (FRA) was defined as the region within the frequency-amplitude space where firing rate exceeded ¼ of the multiunit's peak firing. The firing threshold was calculated as the lowest sound intensity at which suprathreshold firing was evoked in the FRA. The characteristic frequency was the center frequency bin at the firing threshold, and corresponds to the tip of the V-shaped FRA. Thresholds and CFs are determined by

custom MATLAB program confirmed by visual inspection. Auditory cortical tonotopic map was reconstructed by Voronoi tessellation (MATLAB, Mathworks).

Statistics

Statistical analyses were conducted using MATLAB and SPSS (IBM). Repeated measures ANOVAs followed by post-hoc t-tests were conducted to evaluate the statistical significance of the differences between groups or experimental procedures. Analysis of covariance (ANCOVA) was used to examine multiunit threshold differences between groups, using the CF as the covariant. Linear correlation between two variables was tested by Pearson correlation. Two-tailed tests were used unless otherwise stated. The significance level was set at $\alpha = 5\%$. Data were presented as mean ± SEM unless otherwise stated.

Appendix 3.1 Figures

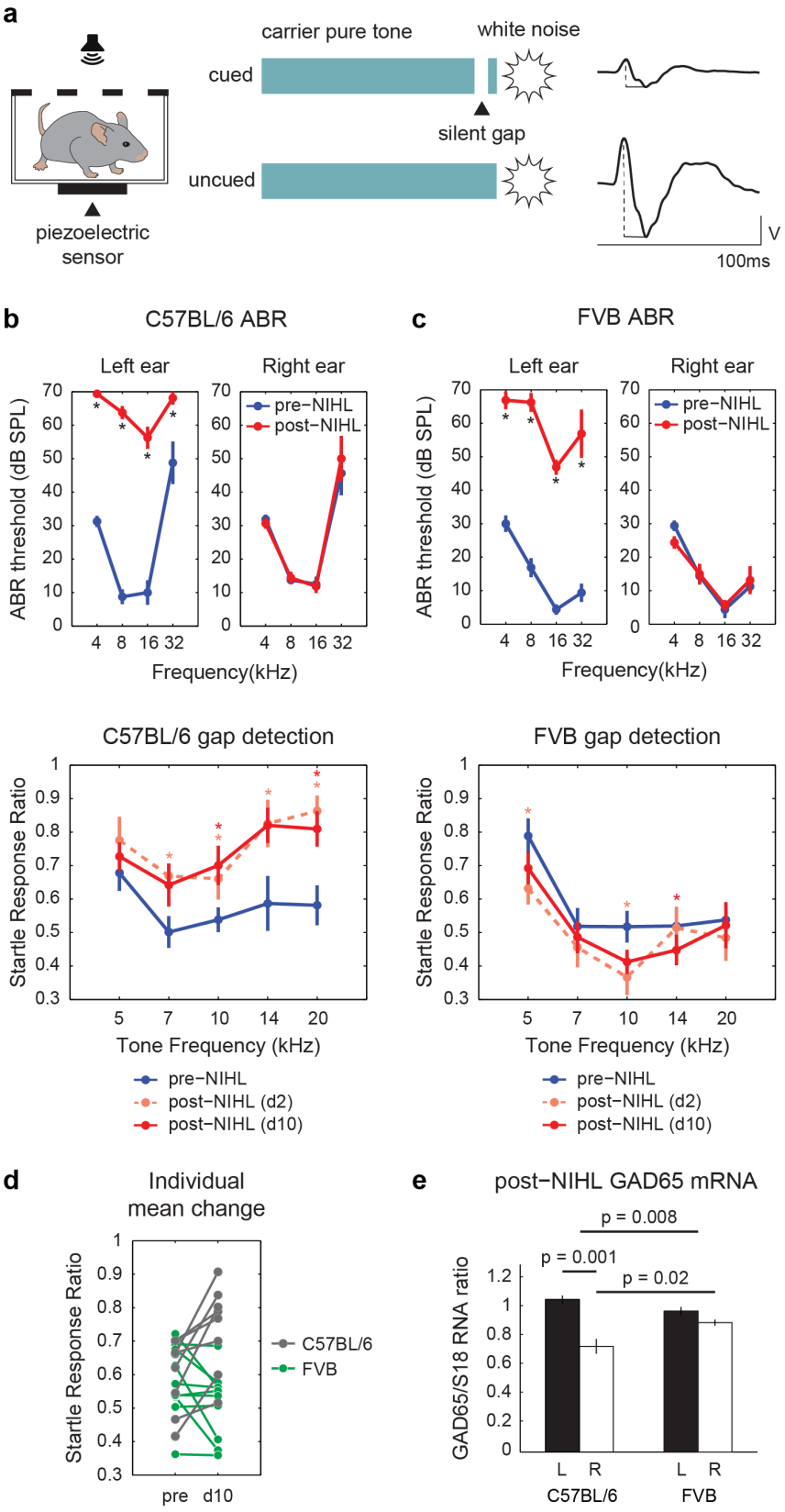

Figure 3.1. Strain differences in gap detection and cortical GAD65 level following noise-induced hearing loss

(**a**) Schematic representation of the gap detection setup (left), sound stimulus (middle), and average startle response trace for cued and uncued trials (right). (**b-c** top) Auditory brainstem response thresholds before and 15-20 days after unilateral NIHL to the left ear in **(b)** C57BL/6 and **(c)** FVB. (**b-c** bottom) Gap detection behavior before, 2 days (d2) after, and 10 days (d10) after NIHL in **(b)** C57BL/6 and **(c)** FVB. Statistical significance was determined by ANOVA followed by a post-hoc paired t-test *$p<0.05$ (**d**) Individual animals' average (tone frequency-collapsed) gap detection behavior for before and 10 days after NIHL. Line color indicates the mouse strain used (gray = C57BL/6, green = FVB) (**e**) Auditory cortex GAD65 mRNA level for C57BL/6 and FVB 10 days after NIHL as measured by the ratio of GAD65 to S18 RNA. Bar color indicates the cortical side (white = right/auditory cortex contralateral to noise-exposed ear, black = left/auditory cortex ipsilateral to noise-exposed ear, in the same animal)

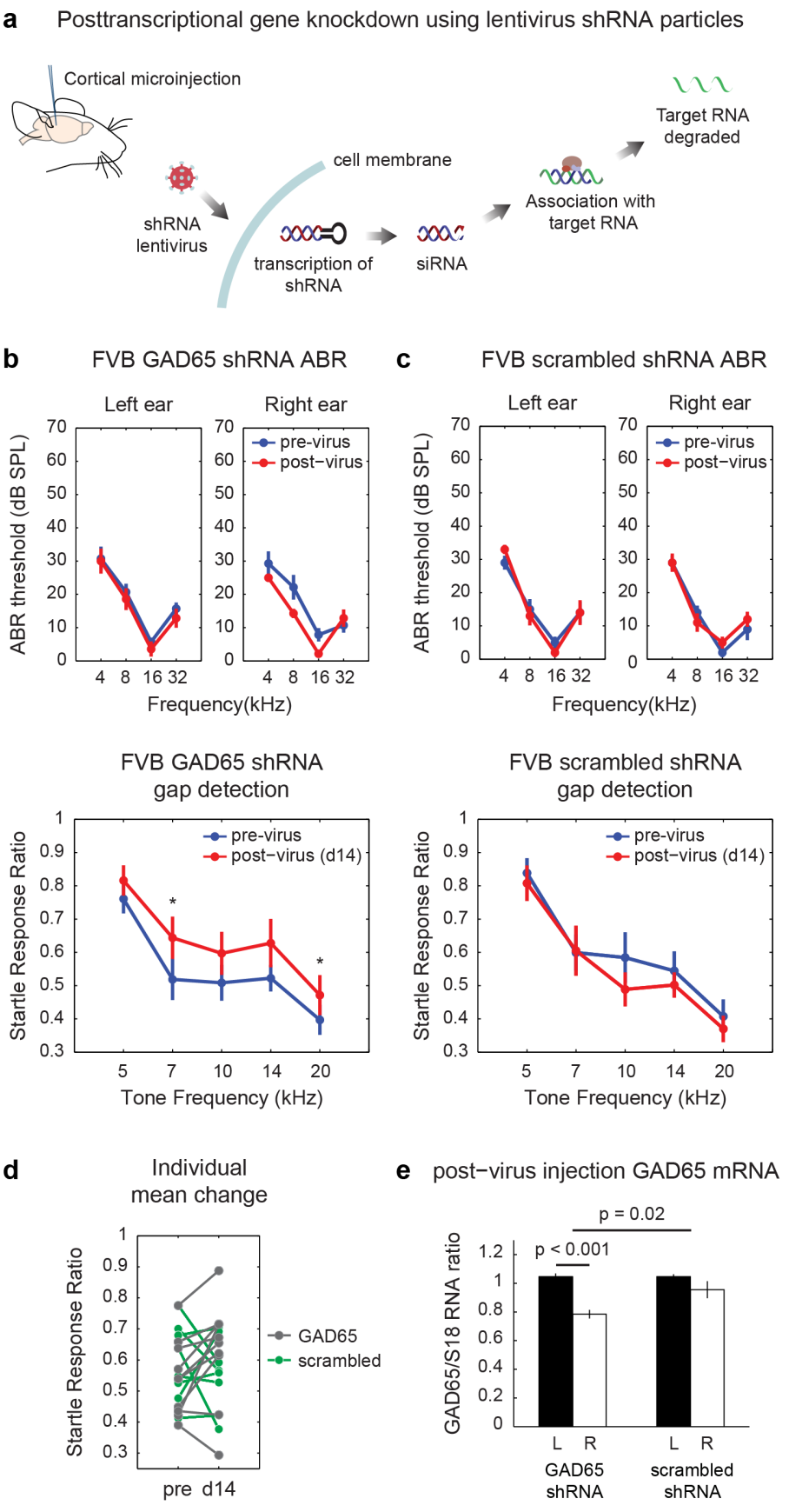
a
Posttranscriptional gene knockdown using lentivirus shRNA particles
Cortical microinjection
shRNA lentivirus
cell membrane
transcription of shRNA
siRNA
Association with target RNA
Target RNA degraded
b
FVB GAD65 shRNA ABR
Left ear
Right ear
ABR threshold (dB SPL)
pre-virus
post-virus
Frequency(kHz)
c
FVB scrambled shRNA ABR
FVB GAD65 shRNA gap detection
FVB scrambled shRNA gap detection
Startle Response Ratio
pre-virus
post-virus (d14)
Tone Frequency (kHz)
d
Individual mean change
GAD65
scrambled
pre d14
e
post-virus injection GAD65 mRNA
p = 0.02
p < 0.001
GAD65/S18 RNA ratio
L R
GAD65 shRNA
scrambled shRNA

Figure 3.2. Cortical GAD65 knockdown in tinnitus-resistant strain is sufficient to induce tinnitus

(**a**) Schematic representation of cortical GAD65 knockdown using shRNA lentiviral particles. (**b-c** top) Auditory brainstem response thresholds before and 15-20 days after injection of **(b)** GAD65 shRNA and **(c)** control scrambled shRNA to the right auditory cortex. (**b-c** bottom) Gap detection behavior before and 14 days (d14) after injection of **(b)** GAD65 shRNA and **(c)** control scrambled shRNA. Statistical significance was determined by ANOVA followed by post-hoc paired t-test *$p<0.05$ (**d**) Individual animal's average (tone frequency-collapsed) gap detection behavior for before and 14 days after shRNA injection. Line color indicates the virus type used (gray = GAD65 shRNA, green = control scrambled shRNA). (**e**) Auditory cortex GAD65 mRNA level 14 days after shRNA injection as measured by the ratio of GAD65 to S18 RNA. Bar color indicates the cortical side (white = right/shRNA injected auditory cortex, black = left/uninjected auditory cortex, in the same animal).

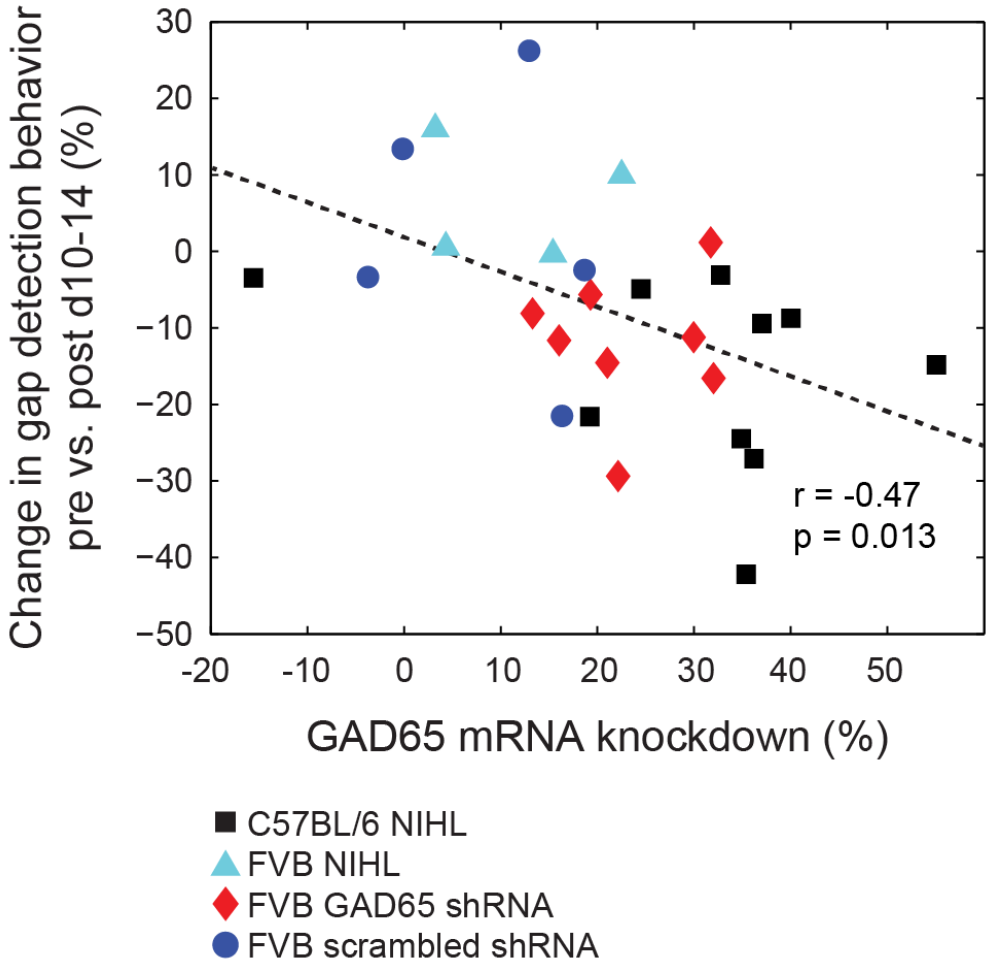

Figure 3.3. Cortical GAD65 reduction correlates with severity of tinnitus

Tinnitus behavior is significantly correlated with reduction in cortical GAD65 mRNA level. The x-axis shows the percent of GAD65 mRNA reduction in the treated/right cortex relative to the intact/left cortex. The y-axis shows the percent change in gap detection behavior before and after the experimental manipulation (i.e., NIHL or shRNA injection). Post-manipulation behavior was assessed at d10 in NIHL case and d14 in shRNA case. Zero-value indicates no change, positive value indicates improvement and negative value indicates impairment. One-tailed Pearson correlation (r = -0.47, n = 27, p = 0.013).

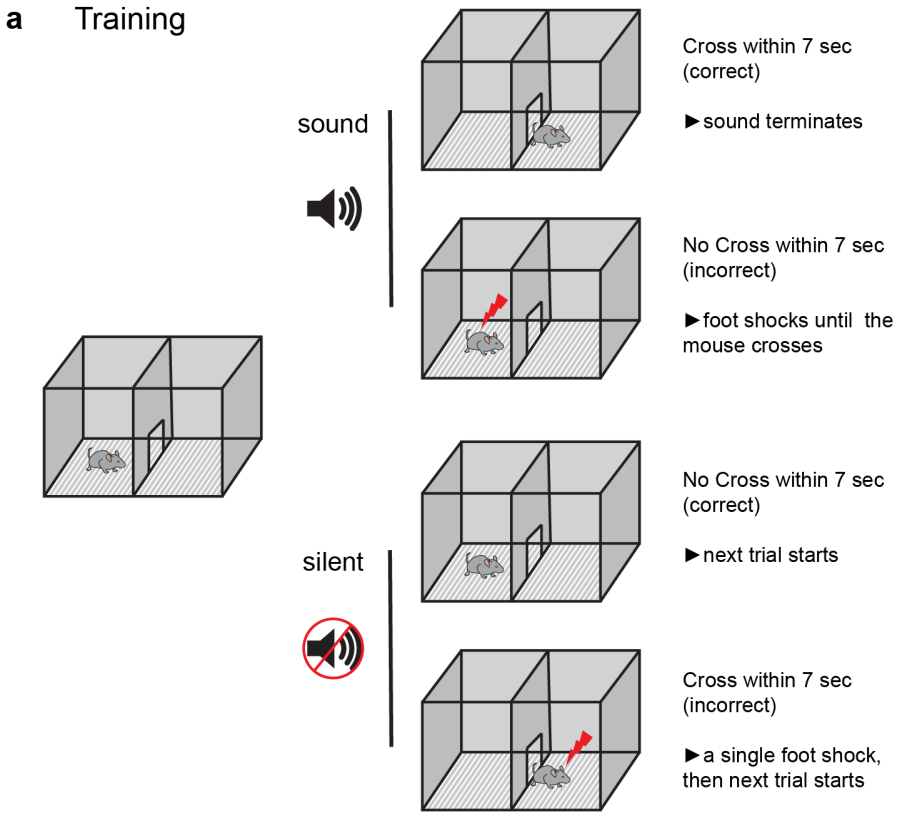
a
Training
sound
silent
Cross within 7 sec
(correct)
►sound terminates
No Cross within 7 sec
(incorrect)
►foot shocks until the
mouse crosses
No Cross within 7 sec
(correct)
►next trial starts
Cross within 7 sec
(incorrect)
►a single foot shock,
then next trial starts

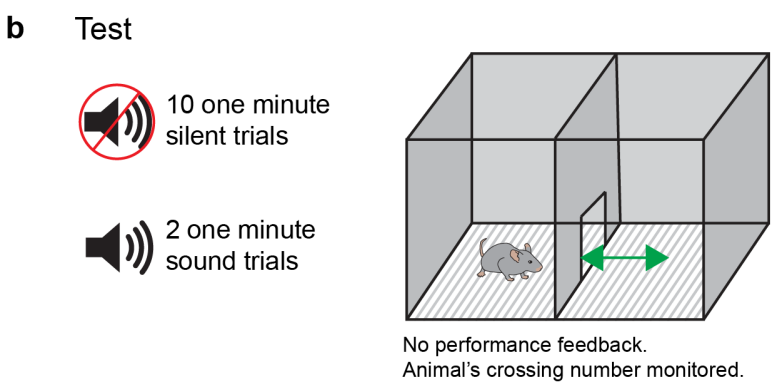
b
Test
10 one minute
silent trials
2 one minute
sound trials
No performance feedback.
Animal's crossing number monitored.

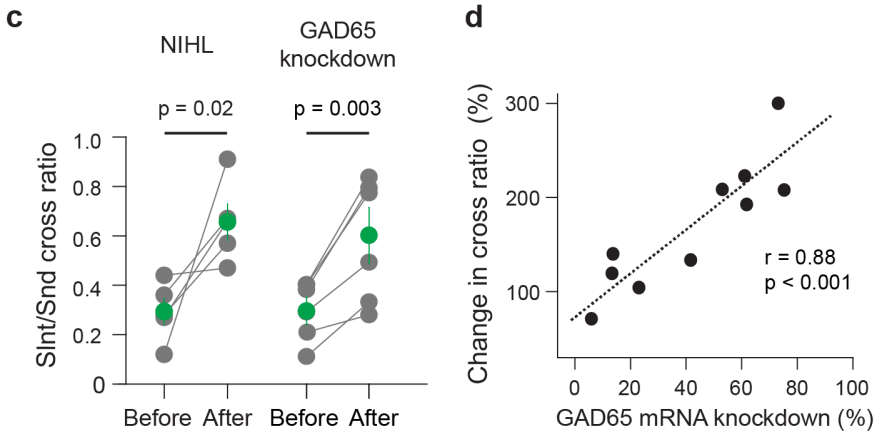
c
NIHL
GAD65
knockdown
p = 0.02
p = 0.003
SInt/Snd cross ratio
1.0
0.8
0.6
0.4
0.2
0
Before After Before After
d
Change in cross ratio (%)
300
200
100
r = 0.88
p < 0.001
0 20 40 60 80 100
GAD65 mRNA knockdown (%)

Figure 3.4. Cortical GAD65 reduction correlates with tinnitus as measured by a conditioned active avoidance task

(a) Schematic representation of the active avoidance task training. Animals were trained on the reinforced trials until they reach 70% overall accuracy. **(b)** Schematic representation of the active avoidance probe (test) trials. 12 unreinforced probe trials were randomly intermixed with 48 reinforced trials in a test session. **(c)** Tinnitus behavior before and after NIHL or cortical GAD65 knockdown (gray = individual mouse, green = group mean of the condition). **(d)** Tinnitus behavior is significantly correlated with cortical GAD65 mRNA knockdown level (one-tailed Pearson correlation, $r = 0.88$, $n = 10$, $p < 0.001$). The x-axis shows the percent of GAD65 mRNA reduction in the injected/right cortex relative to the uninjected/left cortex. The y-axis shows the percent change in tinnitus behavior between before and after GAD65 knockdown.

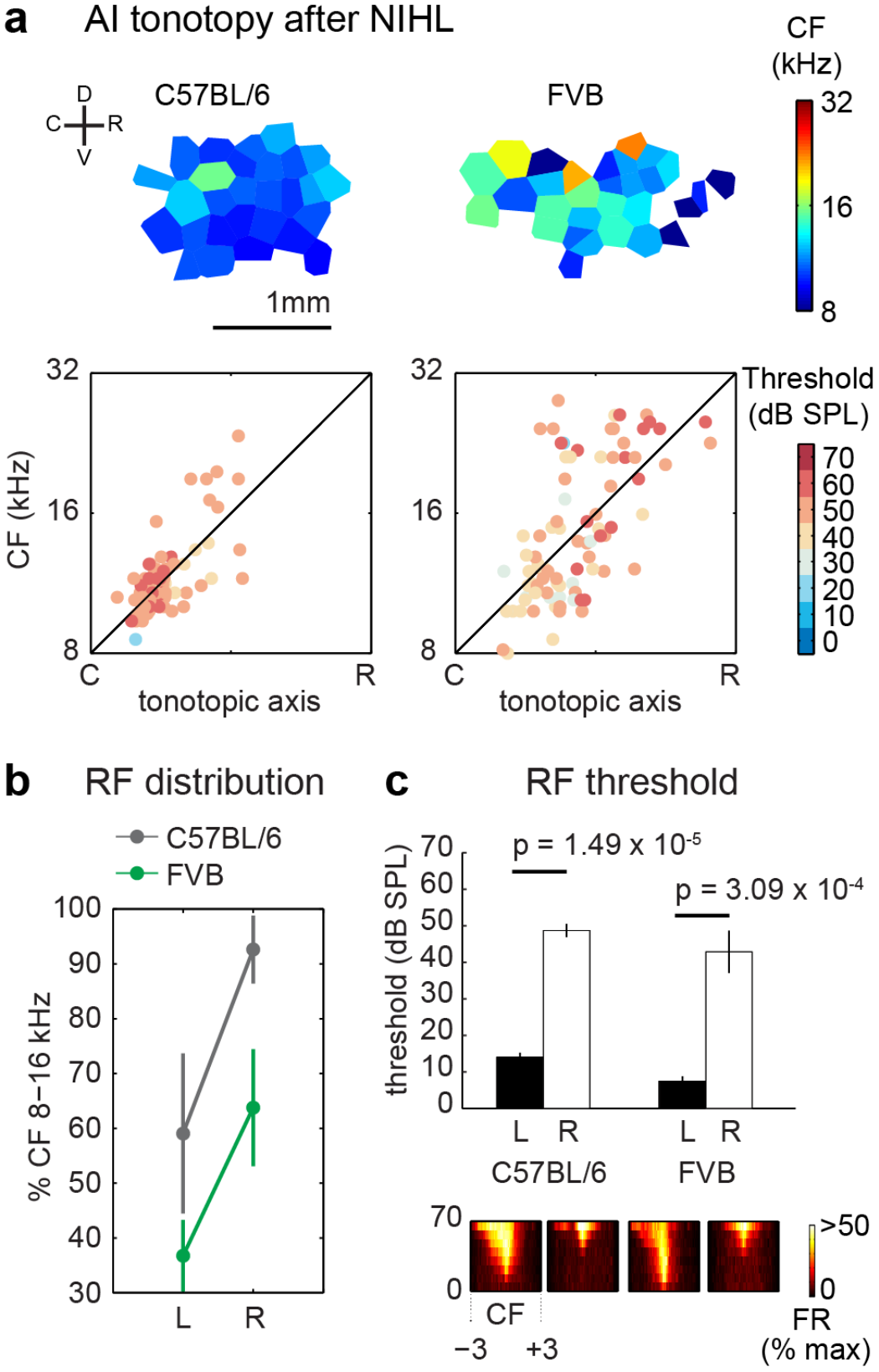
a
AI tonotopy after NIHL
C57BL/6
FVB
D
C
R
V
1mm
CF (kHz)
32
16
8
CF (kHz)
tonotopic axis
Threshold (dB SPL)
70
60
50
40
30
20
10
0
b
RF distribution
C57BL/6
FVB
% CF 8–16 kHz
100
90
80
70
60
50
40
30
L
R
c
RF threshold
p = 1.49 x 10-5
p = 3.09 x 10-4
threshold (dB SPL)
C57BL/6
FVB
>50
FR
(% max)
CF
−3
+3

Figure 3.5. NIHL causes AI reorganization and increases firing threshold in both C57BL/6 and FVB

(a) Top: Example AI frequency maps of C57BL/6 and FVB after NIHL. Bottom: Characteristic frequency distribution of all subjects along the caudal-rostral (C-R) extent of AI. Dot color indicates firing threshold of each multiunit. **(b)** Percentage of 8-16 kHz tuned sites in AI, segregated by strain (gray = C57BL/6, green = FVB) and cortical sides (L = left/auditory cortex ipsilateral to noise-exposed ear, R = right/auditory cortex contralateral to noise-exposed ear, in the same animal). **(c)** Top: Response threshold for two strains and cortical sides. Bottom: CF-centered average receptive fields of AI multiunit for all subjects in each condition. The colorbar indicates firing rate normalized to the peak firing at each multiunit. The x-axis indicates octave distance from the CF (center) of each multiunit. The y-axis indicates sound amplitude in dB SPL.

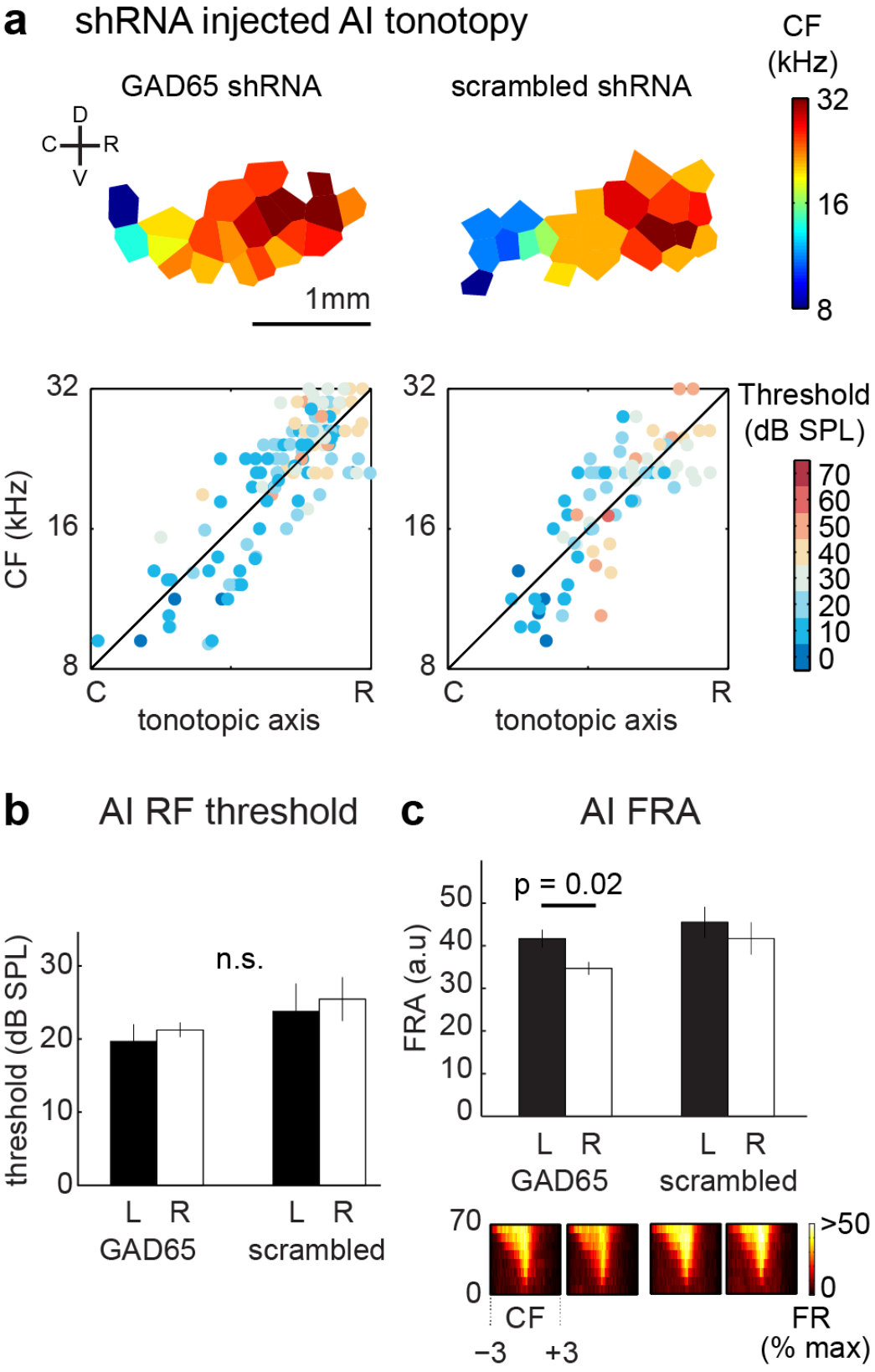
a
shRNA injected AI tonotopy
GAD65 shRNA
scrambled shRNA
CF (kHz)
32
16
8
D
C
R
V
1mm
32
16
8
CF (kHz)
C
R
tonotopic axis
Threshold (dB SPL)
70
60
50
40
30
20
10
0
b
AI RF threshold
threshold (dB SPL)
30
20
10
0
n.s.
L R
GAD65
L R
scrambled
c
AI FRA
p = 0.02
FRA (a.u)
50
40
30
20
10
0
L R
GAD65
L R
scrambled
70
0
CF
−3 +3
>50
0
FR
(% max)

Figure 3.6. GAD65 knockdown does not affect AI tonotopy but decreases receptive field size

(a) Top: Example AI frequency maps of FVB after injection of virus carrying GAD65 shRNA or scrambled shRNA. Bottom: Characteristic frequency distribution of all subjects along the caudal-rostral (C-R) extent of AI. Dot color indicates firing threshold of each multiunit. **(b)** Response threshold for two groups and cortical sides. N.s., not significant. **(c)** Top: Quantification of AI frequency responsive area (FRA) for two groups and cortical sides. Bottom: CF-centered average receptive fields of AI multiunit for all subjects in each condition. The colorbar indicates firing rate normalized to the peak firing at each multiunit. The x-axis indicates octave distance from the CF (center) of each multiunit. The y-axis indicates sound amplitude (dB SPL).

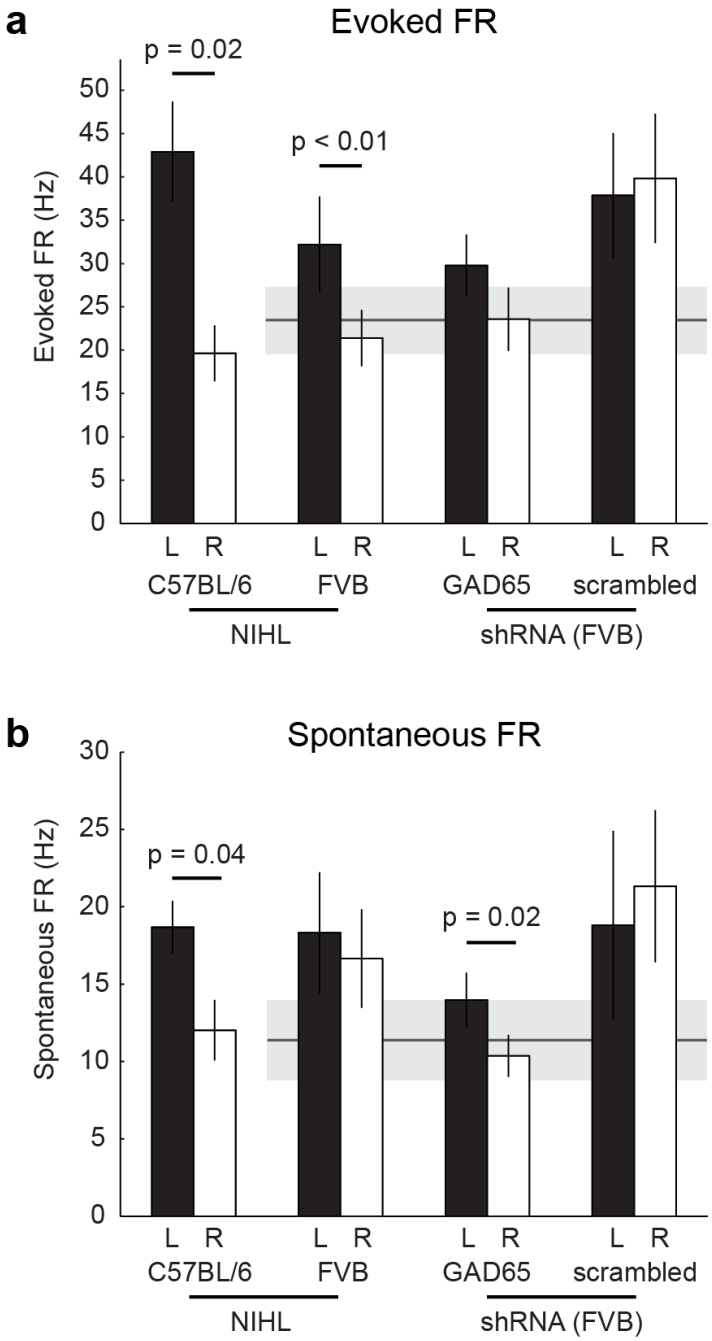

Figure 3.7. GAD65 downregulation decreases AI spontaneous firing while NIHL reduces AI evoked firing

Quantification of **(a)** evoked firing rate and **(b)** spontaneous firing rate in four groups and two cortical sides. R = right cortex is the target of manipulation in both NIHL and shRNA experiments. L = left cortex in the same animal. Black line and surrounding gray shading in the background indicates mean ± SEM of the firing rate for **(a)** evoked or **(b)** spontaneous conditions in naïve FVB (n=6, reanalysis of a previously published dataset (Kim, Gibboni et al. 2013)).

Table 3.1. Summary of Results

Strain	Treatment	Tinnitus	Hearing loss	Map change	Evoked FR	Spontaneous FR	GAD65
C57BL/6J	NIHL	+	+	+	+↓	+↓	+↓
FVB.129P2-*Pde6b*+ *Tyrc-ch*/AntJ	NIHL	-	+	+	+↓	-	-
FVB.129P2-*Pde6b*+ *Tyrc-ch*/AntJ	GAD65 shRNA	+	-	-	-	+↓	+↓
FVB.129P2-*Pde6b*+ *Tyrc-ch*/AntJ	scrambled shRNA	-	-	-	-	-	-
Tg(dlx6a-cre)1Mekk	NIHL	+	+	N/A	N/A	N/A	+↓
Tg(dlx6a-cre)1Mekk	GAD65 shRNA	+	-	N/A	N/A	N/A	+↓

Positive sign (+) indicates the presence of a statistically significant difference compared to the appropriate control condition. Negative sign (-) indicates the absence of a statistically significant difference compared to the control condition. When applicable, the direction of the positive result is indicated with an arrow. Down arrow (↓) indicates a reduction. N/A indicates data not available.

Appendix 3.2 Supplemental Information

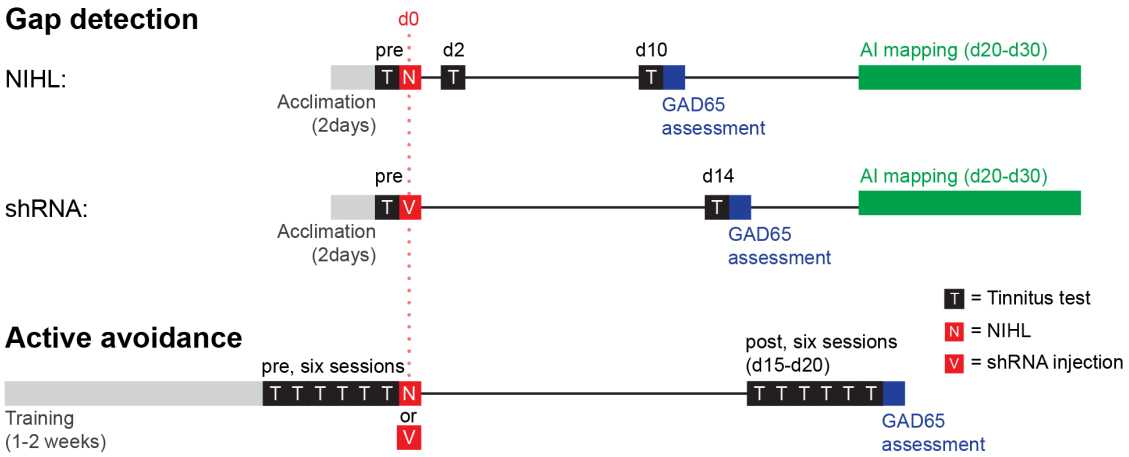

Figure 3S.1. Summary and timeline of all experiments

T = tinnitus test; N = NIHL; V = shRNA lentivirus injection. Black squares indicate acquisition of the behavior data included in the analysis.

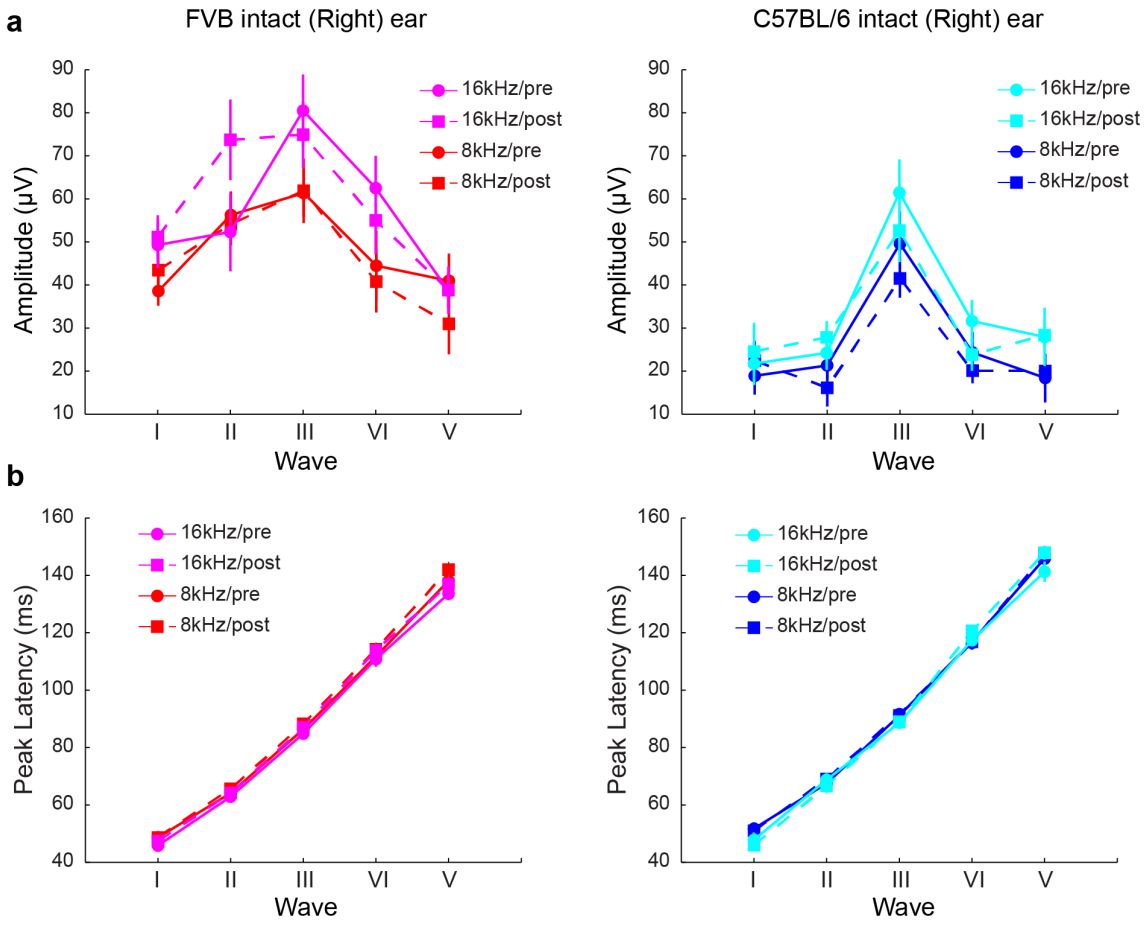

Figure 3S.2. ABR wave amplitude and peak latency of the protected ear are unaffected by NIHL

Successful unilateral NIHL was confirmed by unchanged **(a)** ABR wave amplitude (ANOVA, session, $F_{1,13} = 0.07$, $p = .79$; session-by-strain interaction, $F_{1,13} = 0.28$. $p = 0.61$) and **(b)** ABR peak latency (ANOVA, session $F_{1,12} = 0.51$, $p = 0.49$; session-by-strain interaction, $F_{1,12} = 0.42$, $p = 0.53$) recorded from the protected (right) ear. ABRs were evaluated at 60dB SPL in FVB (n = 8) and C57BL/6 (n = 8), 15-20 days after NIHL.

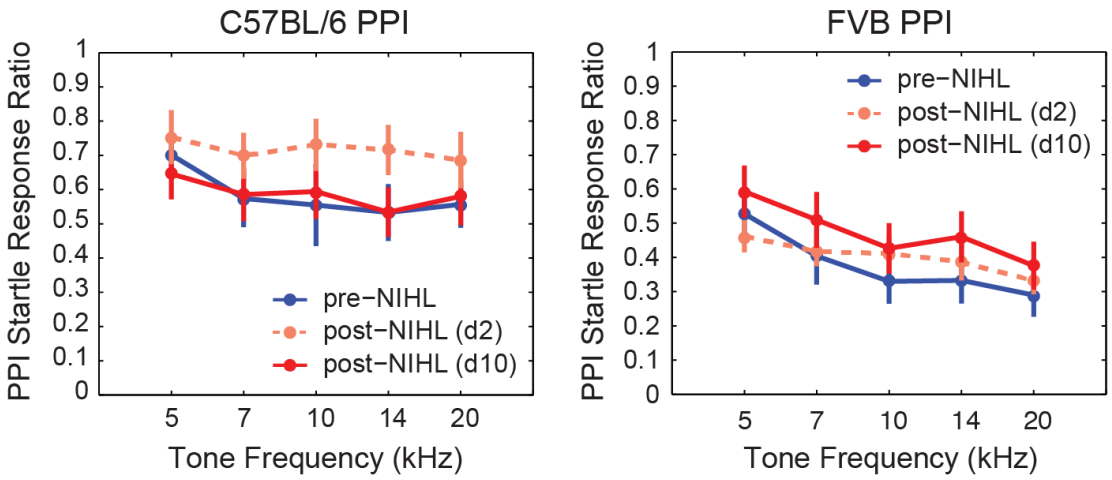

Figure 3S.3. Pre-pulse inhibition (PPI) is unaffected by NIHL in both C57BL/6 and FVB

NIHL did not affect PPI in both C57BL/6 (n = 7) and FVB (n = 7) (ANOVA, session, $F_{2,11} = 1.58$, $p = 0.25$). In addition, no strain difference was observed (ANOVA, session-by-strain interaction, $F_{2,11} = 2.7$, $p = 0.11$).

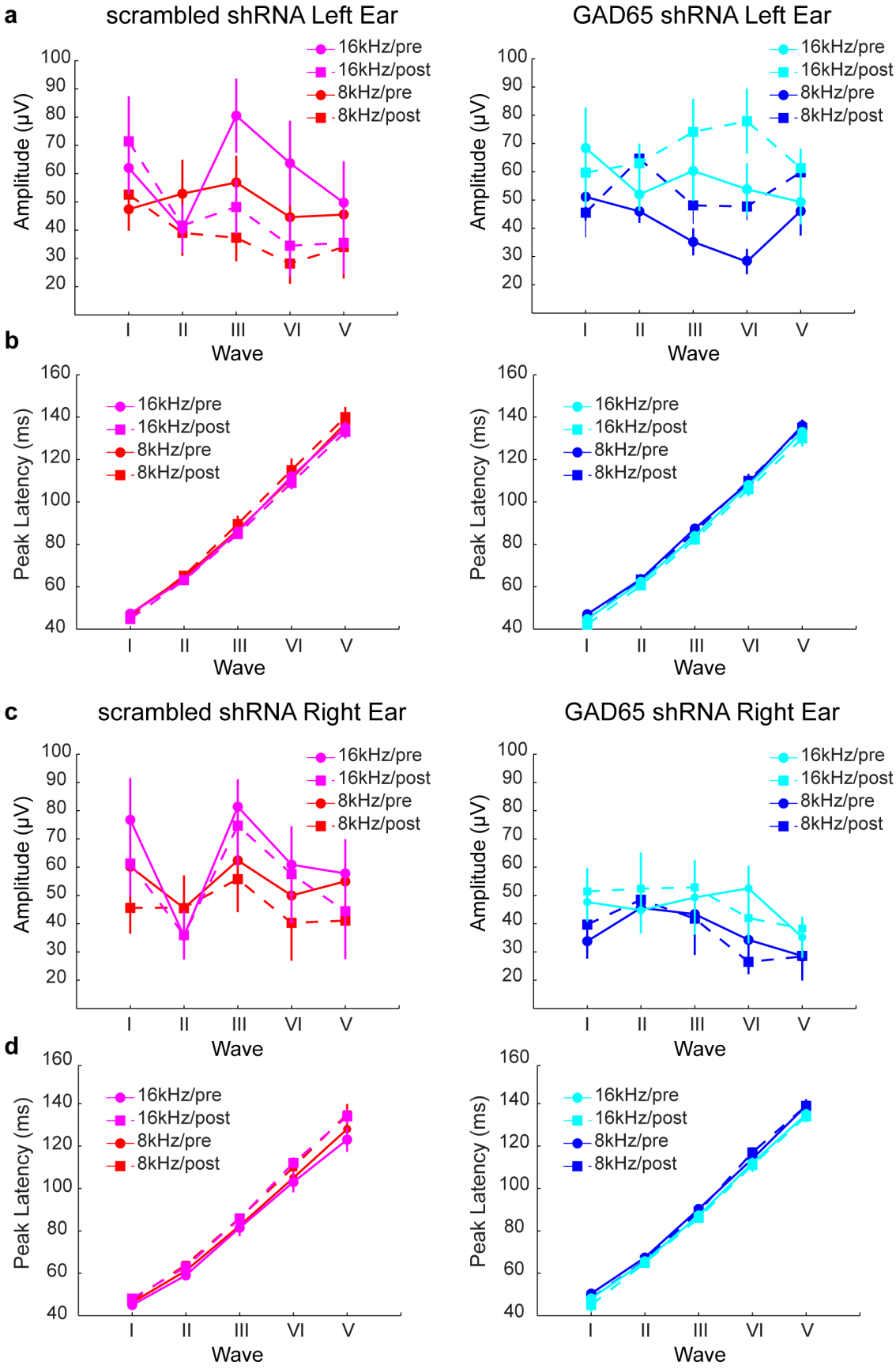
a
scrambled shRNA Left Ear
GAD65 shRNA Left Ear
16kHz/pre
16kHz/post
8kHz/pre
8kHz/post
Amplitude (μV)
Wave
b
Peak Latency (ms)
c
scrambled shRNA Right Ear
GAD65 shRNA Right Ear
d

Figure 3S.4. ABR wave amplitude and peak latency are unaffected by virus injection

shRNA lentivirus particle injection did not affect ABR wave amplitude (ANOVA, session $F_{1,10} = 0.37$, $p = 0.65$; session-by-virus type interaction, $F_{1,10} = 7.73$, $p = 0.06$; session-by-virus type-by-ear interaction, $F_{1,10} = 1.16$, $p = 0.31$) and peak latency (ANOVA, session $F_{1,10} = 0.36$, $p = 0.56$; session-by-virus type interaction, $F_{1,10} = 2.34$, $p = 0.16$; session-by-virus type-by-ear interaction, $F_{1,10} = 0.65$, $p = 0.44$) in **(a-b)** left and **(c-d)** right ear. Injection was conducted in right auditory cortex. ABRs were evaluated at 60dB SPL, 15-20 days after injection, in FVB with GAD65 shRNA injection (n = 7) and scrambled shRNA injection (n = 5).

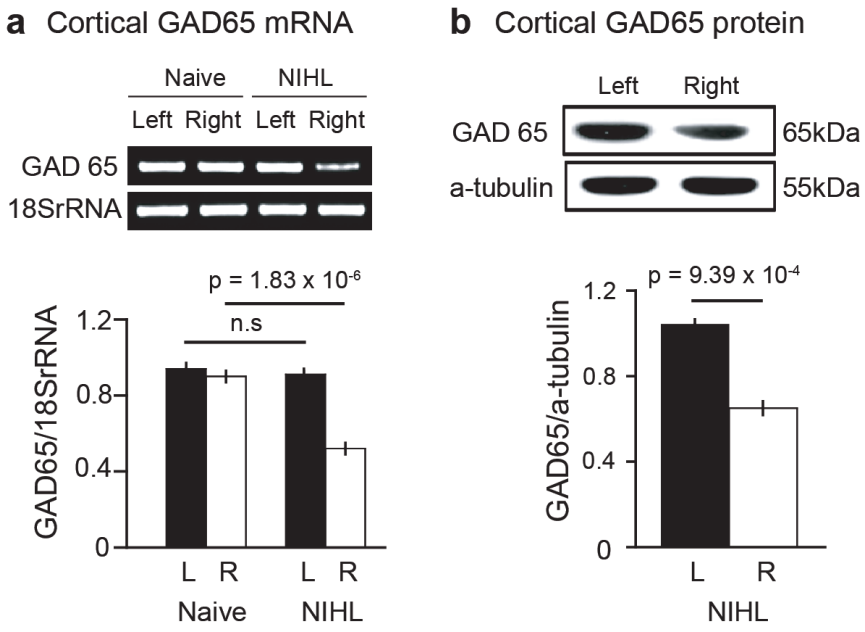

Figure 3S.5. Tg(dlx6a-cre)1Mekk) mice shows NIHL-induced downregulation of GAD65 mRNA and protein

Bilateral cortical GAD65 mRNA expression in naïve (n = 5), and noise-exposed (n = 5) Tg(dlx6a-cre)1Mekk) mice was analyzed with RT-PCR. RT-PCR was conducted 21 days after the previously described NIHL procedure to the left ear or a sham NIHL procedure. GAD65 protein level was also analyzed 15 days after NIHL with Western blot (n = 3). **(a)** Downregulation of GAD65 mRNA was observed in the NIHL-affected (right) auditory cortex (ANOVA, $F_{1,14} = 59.2$, $p < 0.01$, post-hoc independent t-test, $t_8 = 23.84$, $p = 1.83 \times 10^{-6}$). GAD65 mRNA level in left auditory cortex (ipsilateral to noise-exposed ear) was not altered compared to naïve animals (ANOVA, $F_{1,14} = 0.16$, $p = 0.69$). **(b)** GAD65 protein levels in the auditory cortex 15 days after NIHL as measured by the ratio of GAD65 to a-tubulin. GAD65 protein level was reduced in the NIHL-affected (right) auditory cortex (ANOVA, $F_{1,4} = 76.6$, $p < 0.01$, post-hoc paired t-test, $t_2 = 8.75$, $p = 9.39 \times 10^{-4}$).

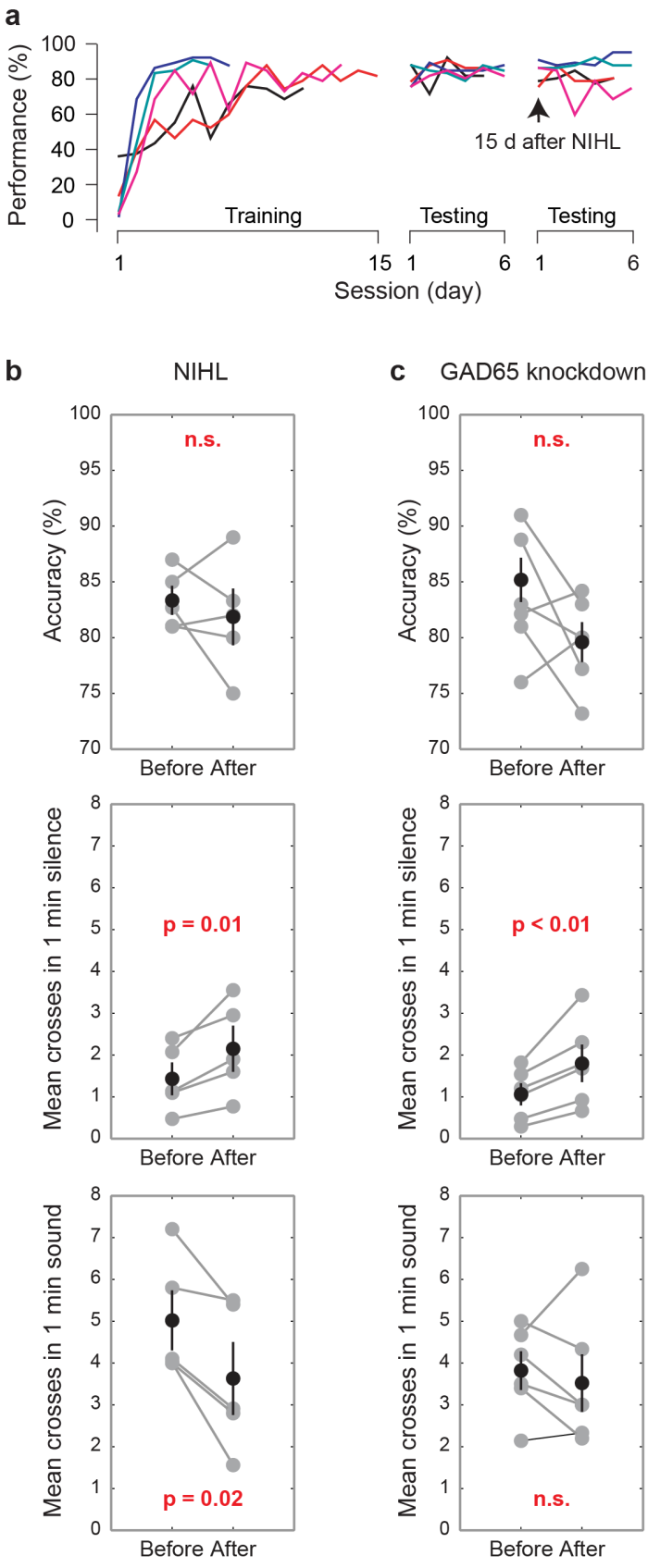
a
Performance (%)
100
80
60
40
20
0
15 d after NIHL
Training
Testing
Testing
1
15
1
6
1
6
Session (day)
b
NIHL
c
GAD65 knockdown
Accuracy (%)
n.s.
Before After
Mean crosses in 1 min silence
p = 0.01
p < 0.01
Mean crosses in 1 min sound
p = 0.02
n.s.

Figure 3S.6. Active avoidance task learning and raw crossing scores

(a) Performance of animals in the active avoidance task during training and testing sessions. Colors indicate different individual animals. **(b)** Top: Average accuracy of the animals on the active avoidance task was not changed by unilateral NIHL. Middle: The number of barrier crosses in silent probe trials significantly increased after NIHL (paired t-test, $p = 0.01$). Bottom: The number of barrier crosses in sound probe trials significantly decreased after NIHL (paired t-test, $p = 0.02$). **(c)** Top: Average accuracy of the animals on the active avoidance task was not changed by GAD65 knockdown in the right auditory cortex. Middle: The number of barrier crosses in silent probe trials significantly increased after GAD65 knockdown (paired t-test, $p < 0.01$). Bottom: The number of barrier crosses in sound probe trials was unchanged after GAD65 knockdown. Gray indicates individual performances, and black indicates group mean of the condition. n.s., not significant.

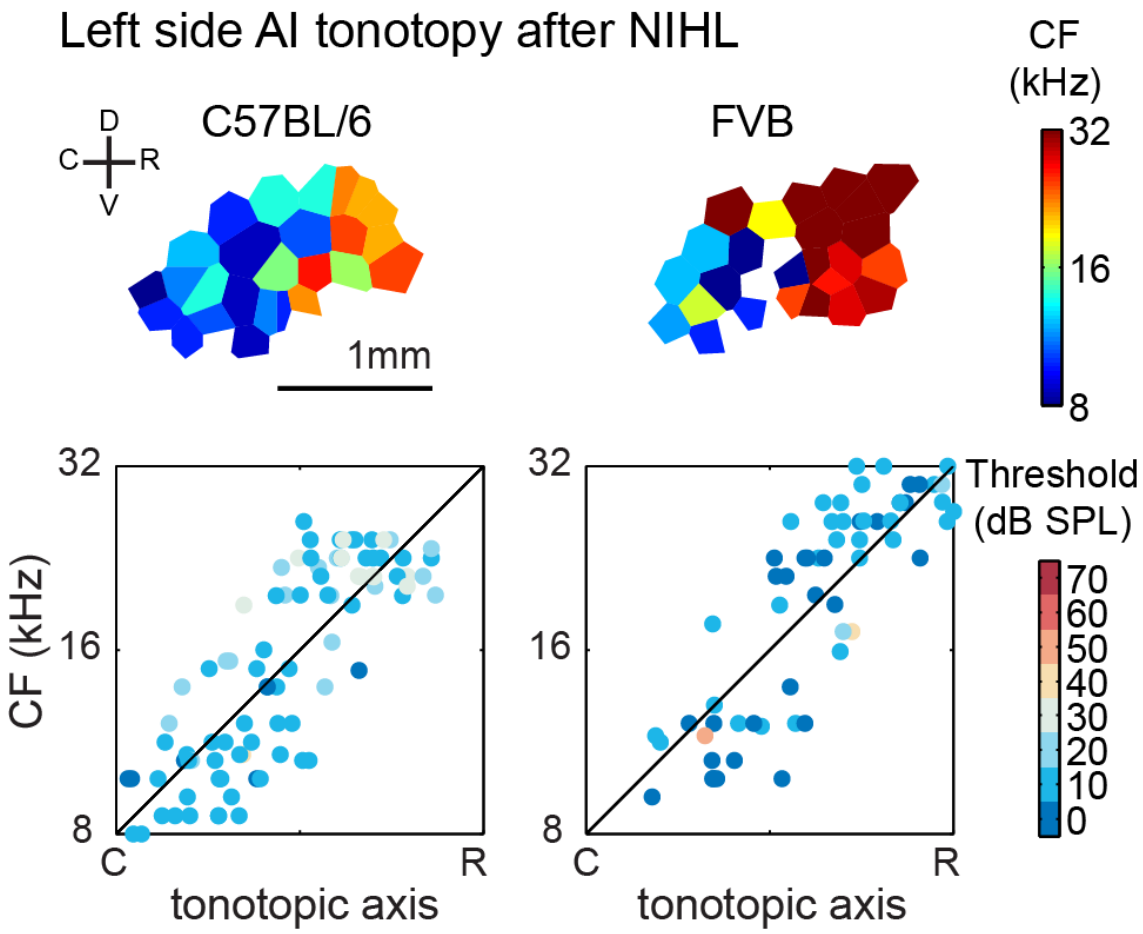

Figure 3S.7. AI ipsilateral to the noise-exposed ear exhibits normal tonotopy and threshold in both strains
Top: Example AI frequency maps of C57BL/6 and FVB in the cortex ipsilateral to the noise-exposed ear. Bottom: Characteristic frequency distribution of all subjects along the caudal-rostral (C-R) extent of AI. Dot color indicates firing threshold of each multiunit.

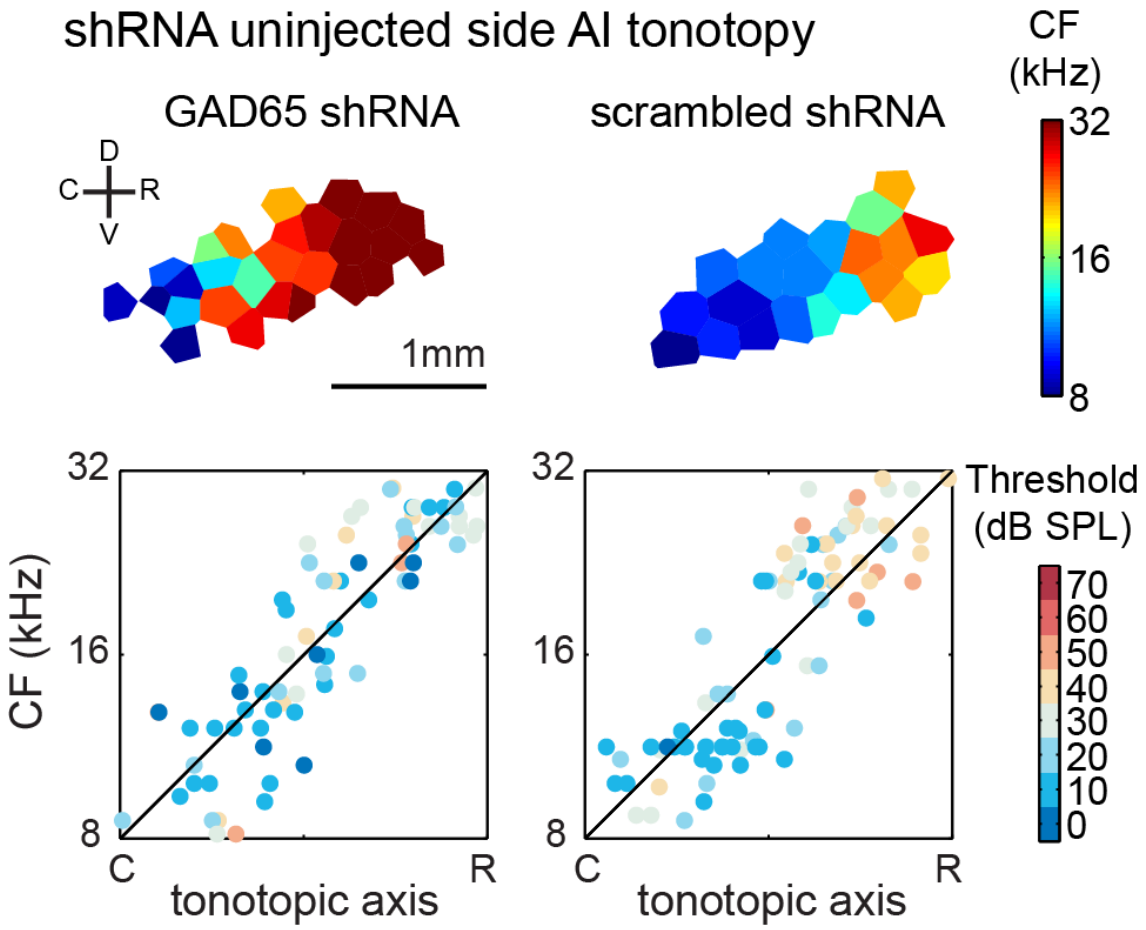

Figure 3S.8. Uninjected AI exhibits normal AI tonotopy and threshold regardless of virus type

Top: Example AI frequency maps of FVB in the uninjected (left) cortex (i.e. cortex contralateral to the virus injection). Bottom: Characteristic frequency distribution of all subjects along the caudal-rostral (C-R) extent of AI. Dot color indicates firing threshold of each multiunit.

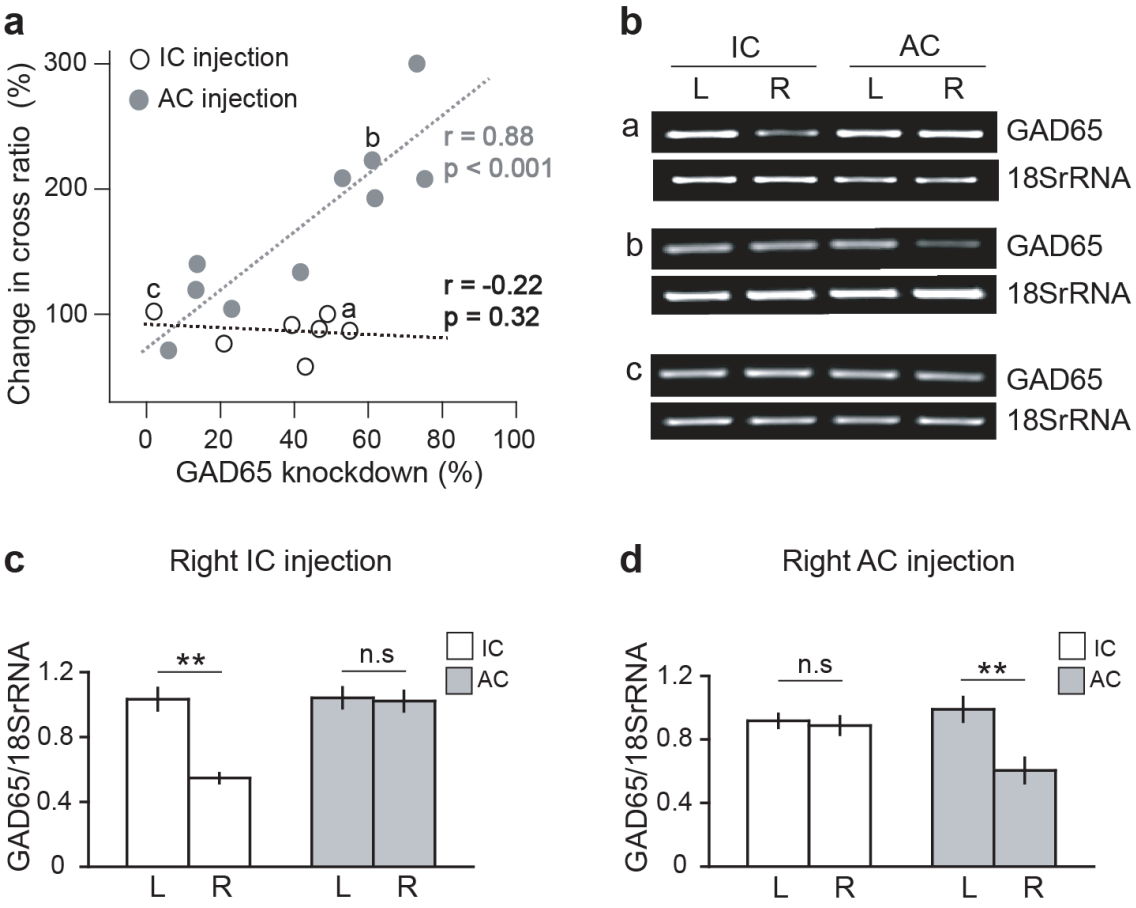

Figure 3S.9. shRNA-mediated GAD65 knockdown is localized in auditory cortex and does not affect inferior colliculus

To test the effect of GAD65 downregulation in inferior colliculus (IC) on tinnitus behavior, additional Tg(dlx6a-cre)1Mekk) mice (n = 7) were injected with GAD65 shRNA in the right IC. GAD65 reduction was assessed relative to the uninjected/left IC, in the same animal. Tinnitus behavior was measured by the active avoidance task. **(a)** Percentage change in the ratio of silent vs. sound crosses as a function of percentage GAD65 knockdown at the injection site (i.e., auditory cortex (AC) or IC). There was a significant positive correlation between the behavioral measure of tinnitus and the GAD65 knockdown level in AC (same as Figure 4D), but not the GAD65 knockdown level in IC (one-tailed Pearson correlation r = -0.22, n = 7, p = 0.32). (**b)** Example GAD65 mRNA expression levels in left (L/uninjected) and right (R/injected) IC and AC of the three animals marked as a, b and c in **a**. (**c-d**) Virus-mediated knockdown of GAD65 is localized to the injected area. Additional Tg(dlx6a-cre)1Mekk were injected with the GAD65 shRNA either in AC (n = 3) or IC (n =5), and GAD65 expression in both AC and IC were analyzed 15 days after the injection. **(c)** Injection of the virus into right IC did not change GAD65 expression in AC. **(d)** Injection of the virus into right AC did not change GAD65 expression in IC. Bar color indicates the tissue type (white = IC, gray = AC). ****, *p*** ≤ 0.01; n.s., not significant.

Chapter 4

Conclusions and opportunities for future research

In my dissertation research, I investigated auditory plasticity in two contexts—during normal development and following hearing loss. Evidences from these studies show that the brain undergoes dynamic functional and structural remodeling throughout life.

In the first study, I showed that the primary auditory cortex and inferior colliculus show different outcomes after the same pure-tone exposure procedure. Tonotopic expansion was observed only in cortex but not in inferior colliculus. While auditory cortex shows lasting effects of tonotopic change into adulthood, inferior colliculus only shows transient narrowing of frequency tuning bandwidth at the exposure frequency. These results, taken together with other reports (Popescu and Polley 2010, Barkat, Polley et al. 2011) suggest that large-scale tonotopic reorganization is unique to cortex and confirms the significant role cortex plays in formation and maintenance of experience-dependent plasticity.

The developmental mechanism that underlies the differential effects observed at cortex and inferior colliculus remains to be investigated in the future. Previous studies showed that the formation of extracelluar matrix proteins, or a perineuronal net, plays an important role in axonal growth regulation and in consolidating sensory cortical circuitry (McRae, Rocco et al. 2007, Balmer, Carels et al. 2009). Interestingly, in the auditory pathway, perineuronal net formation occurs bottom-up: in brainstem at around P4, in ICC at P8, and in AI at P18 (Friauf 2000). One possible explanation for current findings is that the inferior colliculus undergoes earlier maturation of perineuronal nets than AI, and thus the tonotopy is less influenced by early-life sensory experiences, which begin at ear canal opening at P12. Further studies of perineuronal net formation timing, and perturbations of the formation process, may shed light onto the cellular mechanism.

In the second study, I investigated adult tonotopic plasticity following hearing loss. The purpose of this study was to test if tonotopic map change is sufficient to cause impairment in gap detection behavior—which is used as a proxy of human tinnitus. I have shown that tonotopic map change is likely to be a consequence of hearing loss and not sufficient to induce tinnitus behavior by itself. Further, I have shown that tinnitus behavior seems to correlate with downregulation of cortical GAD65 expression—a gene involved in inhibitory neurotransmission. These findings indicate that tinnitus etiology involves an imbalance between excitatory and inhibitory tones in the cortex and suggest a possible therapeutic target for tinnitus. Future studies should test whether it is possible to rescue the tinnitus behavior by manipulating the inhibition of the auditory cortex.

Throughout my dissertation research, I have investigated a small number of auditory regions at a time. This approach has its limitations since it studies regions of interest in isolation, and discounts the role played by extensive interconnectivity within the auditory pathway. For example, AI tonotopy may be driven both by feedforward input from upstream auditory areas but also maintained by feedback from downstream auditory cortical regions (Schreiner and Winer 2007). In addition, auditory cortex sends long-range feedback projections to lower auditory nuclei (Brodal 1972, Takayanagi and Ojima 2006, Winer 2006), as far back as the cochlea (Weedman and Ryugo 1996). Plasticity of AI is unlikely to occur in isolation, and probably has a system-wide impact due to its high interconnectivity. Pathway-wide analysis is logistically and technologically challenging and neuroscience labs traditionally specialize in a small number of auditory regions. I am hopeful that new techniques, like optogenetics combined with cell-type specific labeling

of long-range feedback fibers, will give us the tools to dissect the complexity of auditory pathway in its entirety in the future.

References

Abbott, S. D., L. F. Hughes, C. A. Bauer, R. Salvi and D. M. Caspary (1999). "Detection of glutamate decarboxylase isoforms in rat inferior colliculus following acoustic exposure." Neuroscience **93**(4): 1375-1381.

Balmer, T. S., V. M. Carels, J. L. Frisch and T. A. Nick (2009). "Modulation of perineuronal nets and parvalbumin with developmental song learning." The Journal of neuroscience : the official journal of the Society for Neuroscience **29**(41): 12878-12885.

Barkat, T. R., D. B. Polley and T. K. Hensch (2011). "A critical period for auditory thalamocortical connectivity." Nature neuroscience **14**(9): 1189-1194.

Bauer, C. A. and T. J. Brozoski (2001). "Assessing tinnitus and prospective tinnitus therapeutics using a psychophysical animal model." J Assoc Res Otolaryngol **2**(1): 54-64.

Brodal, P. (1972). "The corticopontine projection in the cat. The projection from the auditory cortex." Archives italiennes de biologie **110**(2): 119-144.

Browne, C. J., J. W. Morley and C. H. Parsons (2012). "Tracking the expression of excitatory and inhibitory neurotransmission-related proteins and neuroplasticity markers after noise induced hearing loss." PLoS One **7**(3): e33272.

Brozoski, T. J. and C. A. Bauer (2005). "The effect of dorsal cochlear nucleus ablation on tinnitus in rats." Hear Res **206**(1-2): 227-236.

Bures, Z., J. Grecova, J. Popelar and J. Syka (2010). "Noise exposure during early development impairs the processing of sound intensity in adult rats." Eur J Neurosci **32**(1): 155-164.

Butler, B. E. and S. G. Lomber (2013). "Functional and structural changes throughout the auditory system following congenital and early-onset deafness: implications for hearing restoration." Frontiers in systems neuroscience **7**: 92.

Caspary, D. M., T. M. Holder, L. F. Hughes, J. C. Milbrandt, R. M. McKernan and D. K. Naritoku (1999). "Age-related changes in GABA(A) receptor subunit composition and function in rat auditory system." Neuroscience **93**(1): 307-312.

Chang, E. F. and M. M. Merzenich (2003). "Environmental noise retards auditory cortical development." Science **300**(5618): 498-502.

Davis, R. R., M. L. Cheever, E. F. Krieg and L. C. Erway (1999). "Quantitative measure of genetic differences in susceptibility to noise-induced hearing loss in two strains of mice." Hear Res **134**(1-2): 9-15.

de Villers-Sidani, E., E. F. Chang, S. Bao and M. M. Merzenich (2007). "Critical period window for spectral tuning defined in the primary auditory cortex (A1) in the rat." J Neurosci **27**(1): 180-189.

Dong, S., W. H. Mulders, J. Rodger and D. Robertson (2009). "Changes in neuronal activity and gene expression in guinea-pig auditory brainstem after unilateral partial hearing loss." Neuroscience **159**(3): 1164-1174.

Dong, S., J. Rodger, W. H. Mulders and D. Robertson (2010). "Tonotopic changes in GABA receptor expression in guinea pig inferior colliculus after partial unilateral hearing loss." Brain Res **1342**: 24-32.

Dracheva, S., S. L. Elhakem, S. R. McGurk, K. L. Davis and V. Haroutunian (2004). "GAD67 and GAD65 mRNA and protein expression in cerebrocortical regions of elderly patients with schizophrenia." J Neurosci Res **76**(4): 581-592.

Eggermont, J. J. (2008). "Role of auditory cortex in noise- and drug-induced tinnitus." Am J Audiol **17**(2): S162-169.

Eggermont, J. J. (2012). "Hearing loss, hyperacusis, or tinnitus: What is modeled in animal research?" Hear Res.

Eggermont, J. J. and L. E. Roberts (2004). "The neuroscience of tinnitus." Trends Neurosci **27**(11): 676-682.

Elgoyhen, A. B. and B. Langguth (2010). "Pharmacological approaches to the treatment of tinnitus." Drug Discov Today **15**(7-8): 300-305.

Engineer, N. D., J. R. Riley, J. D. Seale, W. A. Vrana, J. A. Shetake, S. P. Sudanagunta, M. S. Borland and M. P. Kilgard (2011). "Reversing pathological neural activity using targeted plasticity." Nature **470**(7332): 101-104.

Esclapez, M., N. J. Tillakaratne, D. L. Kaufman, A. J. Tobin and C. R. Houser (1994). "Comparative localization of two forms of glutamic acid decarboxylase and their mRNAs in rat brain supports the concept of functional differences between the forms." J Neurosci **14**(3 Pt 2): 1834-1855.

Flor, H., T. Elbert, S. Knecht, C. Wienbruch, C. Pantev, N. Birbaumer, W. Larbig and E. Taub (1995). "Phantom-limb pain as a perceptual correlate of cortical reorganization following arm amputation." Nature **375**(6531): 482-484.

Fournier, P. and S. Hebert (2013). "Gap detection deficits in humans with tinnitus as assessed with the acoustic startle paradigm: does tinnitus fill in the gap?" Hear Res **295**: 16-23.

Friauf, E. (2000). "Development of chondroitin sulfate proteoglycans in the central auditory system of rats correlates with acquisition of mature properties." Audiology & neuro-otology **5**(5): 251-262.

Gao, E. and N. Suga (1998). "Experience-dependent corticofugal adjustment of midbrain frequency map in bat auditory system." Proc Natl Acad Sci U S A **95**(21): 12663-12670.

Gao, E. and N. Suga (2000). "Experience-dependent plasticity in the auditory cortex and the inferior colliculus of bats: role of the corticofugal system." Proc Natl Acad Sci U S A **97**(14): 8081-8086.

Grecova, J., Z. Bures, J. Popelar, D. Suta and J. Syka (2009). "Brief exposure of juvenile rats to noise impairs the development of the response properties of inferior colliculus neurons." Eur J Neurosci **29**(9): 1921-1930.

Han, Y. K., H. Kover, M. N. Insanally, J. H. Semerdjian and S. Bao (2007). "Early experience impairs perceptual discrimination." Nat Neurosci **10**(9): 1191-1197.

Heffner, H. E. and G. Koay (2005). "Tinnitus and hearing loss in hamsters (Mesocricetus auratus) exposed to loud sound." Behav Neurosci **119**(3): 734-742.

Henry, J. A., K. C. Dennis and M. A. Schechter (2005). "General review of tinnitus: prevalence, mechanisms, effects, and management." J Speech Lang Hear Res **48**(5): 1204-1235.

Huang, Z. J., A. Kirkwood, T. Pizzorusso, V. Porciatti, B. Morales, M. F. Bear, L. Maffei and S. Tonegawa (1999). "BDNF regulates the maturation of inhibition and the critical period of plasticity in mouse visual cortex." Cell **98**(6): 739-755.

Insanally, M. N., H. Kover, H. Kim and S. Bao (2009). "Feature-dependent sensitive periods in the development of complex sound representation." J Neurosci **29**(17): 5456-5462.

Kaltenbach, J. A. (2011). "Tinnitus: Models and mechanisms." Hear Res **276**(1-2): 52-60.

Kandler, K., A. Clause and J. Noh (2009). "Tonotopic reorganization of developing auditory brainstem circuits." Nature neuroscience **12**(6): 711-717.

Kash, S. F., R. S. Johnson, L. H. Tecott, J. L. Noebels, R. D. Mayfield, D. Hanahan and S. Baekkeskov (1997). "Epilepsy in mice deficient in the 65-kDa isoform of glutamic acid decarboxylase." Proc Natl Acad Sci U S A **94**(25): 14060-14065.

Kern, A., C. Heid, W.-H. Steeb, N. Stoop and R. Stoop (2008). "Biophysical parameters modification could overcome essential hearing gaps." PLoS computational biology **4**(8): e1000161.

Kim, H. and S. Bao (2009). "Selective increase in representations of sounds repeated at an ethological rate." J Neurosci **29**(16): 5163-5169.

Kim, H., R. Gibboni, C. Kirkhart and S. Bao (2013). "Impaired critical period plasticity in primary auditory cortex of fragile x model mice." J Neurosci **33**(40): 15686-15692.

Komiya, H. and J. J. Eggermont (2000). "Spontaneous firing activity of cortical neurons in adult cats with reorganized tonotopic map following pure-tone trauma." Acta Otolaryngol **120**(6): 750-756.

Kotak, V. C., S. Fujisawa, F. A. Lee, O. Karthikeyan, C. Aoki and D. H. Sanes (2005). "Hearing loss raises excitability in the auditory cortex." J Neurosci **25**(15): 3908-3918.

Kujawa, S. G. and M. C. Liberman (2009). "Adding insult to injury: cochlear nerve degeneration after "temporary" noise-induced hearing loss." J Neurosci **29**(45): 14077-14085.

Kvestad, E., N. Czajkowski, B. Engdahl, H. J. Hoffman and K. Tambs (2010). "Low heritability of tinnitus: results from the second Nord-Trondelag health study." Arch Otolaryngol Head Neck Surg **136**(2): 178-182.

Langers, D. R., E. de Kleine and P. van Dijk (2012). "Tinnitus does not require macroscopic tonotopic map reorganization." Front Syst Neurosci **6**: 2.

Langguth, B., P. M. Kreuzer, T. Kleinjung and D. De Ridder (2013). "Tinnitus: causes and clinical management." Lancet Neurol **12**(9): 920-930.

Liberman, M. C. and N. Y. Kiang (1978). "Acoustic trauma in cats. Cochlear pathology and auditory-nerve activity." Acta Otolaryngol Suppl **358**: 1-63.

Llano, D. A., J. Turner and D. M. Caspary (2012). "Diminished cortical inhibition in an aging mouse model of chronic tinnitus." J Neurosci **32**(46): 16141-16148.

Lobarinas, E., S. H. Hayes and B. L. Allman (2013). "The Gap-Startle paradigm for tinnitus screening in animal models: Limitations and optimization." Hear Res.

Lobarinas, E., W. Sun, R. Cushing and R. Salvi (2004). "A novel behavioral paradigm for assessing tinnitus using schedule-induced polydipsia avoidance conditioning (SIP-AC)." Hear Res **190**(1-2): 109-114.

Lockwood, A. H., R. J. Salvi and R. F. Burkard (2002). "Tinnitus." N Engl J Med **347**(12): 904-910.

Longenecker, R. J. and A. V. Galazyuk (2011). "Development of tinnitus in CBA/CaJ mice following sound exposure." J Assoc Res Otolaryngol **12**(5): 647-658.

McRae, P. A., M. M. Rocco, G. Kelly, J. C. Brumberg and R. T. Matthews (2007). "Sensory deprivation alters aggrecan and perineuronal net expression in the mouse barrel cortex." The Journal of neuroscience : the official journal of the Society for Neuroscience **27**(20): 5405-5413.

Merzenich, M. M., R. J. Nelson, M. P. Stryker, M. S. Cynader, A. Schoppmann and J. M. Zook (1984). "Somatosensory cortical map changes following digit amputation in adult monkeys." The Journal of comparative neurology **224**(4): 591-605.

Middleton, J. W., T. Kiritani, C. Pedersen, J. G. Turner, G. M. Shepherd and T. Tzounopoulos (2011). "Mice with behavioral evidence of tinnitus exhibit dorsal cochlear

nucleus hyperactivity because of decreased GABAergic inhibition." Proc Natl Acad Sci U S A **108**(18): 7601-7606.

Milbrandt, J. C., T. M. Holder, M. C. Wilson, R. J. Salvi and D. M. Caspary (2000). "GAD levels and muscimol binding in rat inferior colliculus following acoustic trauma." Hear Res **147**(1-2): 251-260.

Mogil, J. S., C. A. Lichtensteiger and S. G. Wilson (1998). "The effect of genotype on sensitivity to inflammatory nociception: characterization of resistant (A/J) and sensitive (C57BL/6J) inbred mouse strains." Pain **76**(1-2): 115-125.

Møller, A. R. (2011). Epidemiology of tinnitus in adults. Textbook of tinnitus. A. R. Møller, B. Langguth, D. Ridder and T. Kleinjung. New York, Springer**:** 29–37.

Moyer, C. E., K. M. Delevich, K. N. Fish, J. K. Asafu-Adjei, A. R. Sampson, K. A. Dorph-Petersen, D. A. Lewis and R. A. Sweet (2012). "Reduced glutamate decarboxylase 65 protein within primary auditory cortex inhibitory boutons in schizophrenia." Biol Psychiatry **72**(9): 734-743.

Muhlnickel, W., T. Elbert, E. Taub and H. Flor (1998). "Reorganization of auditory cortex in tinnitus." Proc Natl Acad Sci U S A **95**(17): 10340-10343.

Norena, A. J. and J. J. Eggermont (2003). "Changes in spontaneous neural activity immediately after an acoustic trauma: implications for neural correlates of tinnitus." Hear Res **183**(1-2): 137-153.

Norena, A. J. and J. J. Eggermont (2005). "Enriched acoustic environment after noise trauma reduces hearing loss and prevents cortical map reorganization." J Neurosci **25**(3): 699-705.

Norena, A. J., G. Moffat, J. L. Blanc, L. Pezard and Y. Cazals (2010). "Neural changes in the auditory cortex of awake guinea pigs after two tinnitus inducers: salicylate and acoustic trauma." Neuroscience **166**(4): 1194-1209.

Oliver, D. L., M. A. Izquierdo and M. S. Malmierca (2011). "Persistent effects of early augmented acoustic environment on the auditory brainstem." Neuroscience **184**: 75-87.

Pace, E. and J. Zhang (2013). "Noise-induced tinnitus using individualized gap detection analysis and its relationship with hyperacusis, anxiety, and spatial cognition." PLoS One **8**(9): e75011.

Patel, A. B., R. A. de Graaf, D. L. Martin, G. Battaglioli and K. L. Behar (2006). "Evidence that GAD65 mediates increased GABA synthesis during intense neuronal activity in vivo." J Neurochem **97**(2): 385-396.

Poon, P. W. and X. Chen (1992). "Postnatal exposure to tones alters the tuning characteristics of inferior collicular neurons in the rat." Brain Research **585**(1-2): 391-394.

Popescu, M. V. and D. B. Polley (2010). "Monaural deprivation disrupts development of binaural selectivity in auditory midbrain and cortex." Neuron **65**(5): 718-731.

Ramachandran, V. S. and D. Rogers-Ramachandran (2000). "Phantom limbs and neural plasticity." Archives of neurology **57**(3): 317-320.

Ranson, A., C. E. Cheetham, K. Fox and F. Sengpiel (2012). "Homeostatic plasticity mechanisms are required for juvenile, but not adult, ocular dominance plasticity." Proc Natl Acad Sci U S A **109**(4): 1311-1316.

Roberts, L. E., J. J. Eggermont, D. M. Caspary, S. E. Shore, J. R. Melcher and J. A. Kaltenbach (2010). "Ringing ears: the neuroscience of tinnitus." J Neurosci **30**(45): 14972-14979.

Saldana, E., M. Feliciano and E. Mugnaini (1996). "Distribution of descending projections from primary auditory neocortex to inferior colliculus mimics the topography of intracollicular projections." J Comp Neurol **371**(1): 15-40.

Salvi, R. J., J. Wang and D. Ding (2000). "Auditory plasticity and hyperactivity following cochlear damage." Hear Res **147**(1-2): 261-274.

Sand, P. G., B. Langguth, J. Itzhacki, A. Bauer, S. Geis, Z. E. Cardenas-Conejo, V. Pimentel and T. Kleinjung (2012). "Resequencing of the auxiliary GABA(B) receptor subunit gene KCTD12 in chronic tinnitus." Front Syst Neurosci **6**: 41.

Sand, P. G., B. Langguth, T. Kleinjung and P. Eichhammer (2007). "Genetics of chronic tinnitus." Prog Brain Res **166**: 159-168.

Sand, P. G., B. Langguth, M. Schecklmann and T. Kleinjung (2012). "GDNF and BDNF gene interplay in chronic tinnitus." Int J Mol Epidemiol Genet **3**(3): 245-251.

Sanes, D. H. and M. Constantine-Paton (1983). "Altered activity patterns during development reduce neural tuning." Science **221**(4616): 1183-1185.

Sanes, D. H. and M. Constantine-Paton (1985). "The sharpening of frequency tuning curves requires patterned activity during development in the mouse, Mus musculus." J Neurosci **5**(5): 1152-1166.

Schaette, R. and R. Kempter (2006). "Development of tinnitus-related neuronal hyperactivity through homeostatic plasticity after hearing loss: a computational model." Eur J Neurosci **23**(11): 3124-3138.

Schreiner, C. E. and J. A. Winer (2007). "Auditory cortex mapmaking: principles, projections, and plasticity." Neuron **56**(2): 356-365.

Seki, S. and J. J. Eggermont (2003). "Changes in spontaneous firing rate and neural synchrony in cat primary auditory cortex after localized tone-induced hearing loss." Hear Res **180**(1-2): 28-38.

Seybold, B. A., A. Stanco, K. K. Cho, G. B. Potter, C. Kim, V. S. Sohal, J. L. Rubenstein and C. E. Schreiner (2012). "Chronic reduction in inhibition reduces receptive field size in mouse auditory cortex." Proc Natl Acad Sci U S A **109**(34): 13829-13834.

Sheikh, S. N., S. B. Martin and D. L. Martin (1999). "Regional distribution and relative amounts of glutamate decarboxylase isoforms in rat and mouse brain." Neurochem Int **35**(1): 73-80.

Son, E. J., L. Wu, H. Yoon, S. Kim, J. Y. Choi and J. Bok (2012). "Developmental gene expression profiling along the tonotopic axis of the mouse cochlea." PloS one **7**(7): e40735.

Sun, W., L. Zhang, J. Lu, G. Yang, E. Laundrie and R. Salvi (2008). "Noise exposure-induced enhancement of auditory cortex response and changes in gene expression." Neuroscience **156**(2): 374-380.

Syka, J., N. Rybalko, J. Mazelova and R. Druga (2002). "Gap detection threshold in the rat before and after auditory cortex ablation." Hear Res **172**(1-2): 151-159.

Takayanagi, M. and H. Ojima (2006). "Microtopography of the dual corticothalamic projections originating from domains along the frequency axis of the cat primary auditory cortex." Neuroscience **142**(3): 769-780.

Takesian, A. E., V. C. Kotak, N. Sharma and D. H. Sanes (2013). "Hearing loss differentially affects thalamic drive to two cortical interneuron subtypes." J Neurophysiol **110**(4): 999-1008.

Tan, J., L. Ruttiger, R. Panford-Walsh, W. Singer, H. Schulze, S. B. Kilian, S. Hadjab, U. Zimmermann, I. Kopschall, K. Rohbock and M. Knipper (2007). "Tinnitus behavior and hearing function correlate with the reciprocal expression patterns of BDNF and Arg3.1/arc in auditory neurons following acoustic trauma." Neuroscience **145**(2): 715-726.

Threlkeld, S. W., S. C. Penley, G. D. Rosen and R. H. Fitch (2008). "Detection of silent gaps in white noise following cortical deactivation in rats." Neuroreport **19**(8): 893-898.

Turner, J. G., T. J. Brozoski, C. A. Bauer, J. L. Parrish, K. Myers, L. F. Hughes and D. M. Caspary (2006). "Gap detection deficits in rats with tinnitus: a potential novel screening tool." Behav Neurosci **120**(1): 188-195.

Van der Loos, H. and T. A. Woolsey (1973). "Somatosensory cortex: structural alterations following early injury to sense organs." Science (New York, NY) **179**(4071): 395-398.

Wang, H., T. J. Brozoski and D. M. Caspary (2011). "Inhibitory neurotransmission in animal models of tinnitus: maladaptive plasticity." Hear Res **279**(1-2): 111-117.

Wang, J., S. L. McFadden, D. Caspary and R. Salvi (2002). "Gamma-aminobutyric acid circuits shape response properties of auditory cortex neurons." Brain Res **944**(1-2): 219-231.

Weedman, D. L. and D. K. Ryugo (1996). "Pyramidal cells in primary auditory cortex project to cochlear nucleus in rat." Brain research **706**(1): 97-102.

Winer, J. A. (2006). "Decoding the auditory corticofugal systems." Hearing research **212**(1-2): 1-8.

Yan, J. and N. Suga (1996). "Corticofugal modulation of time-domain processing of biosonar information in bats." Science **273**(5278): 1100-1103.

Yang, G., E. Lobarinas, L. Zhang, J. Turner, D. Stolzberg, R. Salvi and W. Sun (2007). "Salicylate induced tinnitus: behavioral measures and neural activity in auditory cortex of awake rats." Hear Res **226**(1-2): 244-253.

Yang, S. and S. Bao (2013). "Homeostatic mechanisms and treatment of tinnitus." Restor Neurol Neurosci **31**(2): 99-108.

Yang, S., W. Su and S. Bao (2012). "Long-term, but not transient, threshold shifts alter the morphology and increase the excitability of cortical pyramidal neurons." J Neurophysiol **108**(6): 1567-1574.

Yang, S., B. D. Weiner, L. S. Zhang, S. J. Cho and S. Bao (2011). "Homeostatic plasticity drives tinnitus perception in an animal model." Proc Natl Acad Sci U S A **108**(36): 14974-14979.

Yu, X., D. H. Sanes, O. Aristizabal, Y. Z. Wadghiri and D. H. Turnbull (2007). "Large-scale reorganization of the tonotopic map in mouse auditory midbrain revealed by MRI." Proc Natl Acad Sci U S A **104**(29): 12193-12198.

Zhang, L. I., S. Bao and M. M. Merzenich (2001). "Persistent and specific influences of early acoustic environments on primary auditory cortex." Nat Neurosci **4**(11): 1123-1130.

Zhang, L. I., H. W. Tao, C. E. Holt, W. A. Harris and M. Poo (1998). "A critical window for cooperation and competition among developing retinotectal synapses." Nature **395**(6697): 37-44.

Zhang, Y. and N. Suga (2005). "Corticofugal feedback for collicular plasticity evoked by electric stimulation of the inferior colliculus." J Neurophysiol **94**(4): 2676-2682.

Zhang, Y., N. Suga and J. Yan (1997). "Corticofugal modulation of frequency processing in bat auditory system." Nature **387**(6636): 900-903.

Zhang, Z., Y. Q. Cai, F. Zou, B. Bie and Z. Z. Pan (2011). "Epigenetic suppression of GAD65 expression mediates persistent pain." Nat Med **17**(11): 1448-1455.

Zheng, Q. Y., K. R. Johnson and L. C. Erway (1999). "Assessment of hearing in 80 inbred strains of mice by ABR threshold analyses." Hear Res **130**(1-2): 94-107.